Impurity states and diffusion in metal grain boundaries

S. M. Klotsman

Institute of Metal Physics, Ural Division of the Academy of Sciences of the USSR, Sverdlovsk
Usp. Fiz. Nauk **160**, 99–139 (January 1990)

The temperature dependences of the coefficients representing preferential grain-boundary diffusion (PGBD), the dependences of the PGBD parameters on excess charges of "atomic probes," and the isotopic effect under the PGBD conditions made it possible to identify the interstitial PGBD mechanism for a number of f.c.c. metals. A new effect common to PGBD in metals, has been found: a kink appears in the temperature dependences of the PGBD coefficients. A novel method utilizing atomic probes which give the spectral information has provided data demonstrating a lower density of conduction electrons and lower dynamic parameters of the cores (interiors) of grain boundaries, has proved the existence of atomic probes in the form of mixed split interstitials in grain boundaries, has provided data on the properties of an adsorption layer adjoining a grain boundary (which is responsible for the kink in the temperature dependences of the PGBD coefficients), and has yielded the characteristics of magnetic phase transitions occurring in two-dimensional regions in the core of a grain boundary and in adjoining layers of the lattice of thickness representing several interatomic distances.

1. INTRODUCTION

One- and two-dimensional defects, such as dislocations and grain boundaries in crystals are continuing to attract the interest of researchers for a number of reasons. Their role in determination of the properties of many real crystals of practical importance is well-known and obvious.

The growing arsenal of experimental and theoretical investigation methods is providing new opportunities for in-depth studies of the structure and properties of these semimicroscopic defects. Finally, very recently, the process in applying in practice the potentialities of high-temperature superconductors has opened up a new field in which the specific properties of grain boundaries determine largely a whole range of properties of these materials. It has been found that the interfaces between grains in ceramic and film samples of high-temperature superconductors have quite different properties from those of the bulk. Whether it is simply due to "contamination" of grain boundaries or due to their special structure, and whether it would be possible to eliminate these effects by purification of polycrystalline high-temperature superconductors or if it will be necessary to grow and use single-crystal high-temperature superconductor materials and devices will depend on the nature and properties of these types of defects in solids.

A considerable difficulty encountered in experimental investigations of one- and two-dimensional defects in solids is due to the fact that the density of specific states of electrons and ions associated with the cores of these defects is very low, so that many of the experimental techniques are unsuitable for the investigation of these physical objects. In metals the situation is further complicated by the fact that conduction electrons screen effectively the perturbing potentials of defects and reduce greatly the geometric dimensions of the perturbed regions around them, which makes it more difficult to obtain additional information on the structure and properties of cores of defects creating such regions.

This makes it particularly important for the method of "atomic probes." If there is some way of localizing certain specific atoms (which can be radioactive or stable isotopes, Mössbauer nuclei, etc.) in the *core* of a structure defect, then such atomic probes can provide a great variety of physical information on their states against a practically nonexistent background in spite of the low density of specific defect states.

One of the earliest applications of the method of atomic probes in investigations of one- and two-dimensional defects is the use of radioactive and stable tracers localized in the cores of these defects, in studies of diffusion phenomena. When atomic probes are used in this way as simply indicators of the diffusion flux, only the macroscopic data are utilized and then models can be used to obtain more or less reliable microscopic representations. Such macroinformation is presented in Sec. 2 of the present review and an analysis is made there of the relevant microscopic models and representations which are not in conflict with such data.

The following comments should be made here. The bulk of the experimental results presented in this review have been obtained for polycrystalline samples. The use of such samples in studies of the average properties of an ensemble of grain boundaries is one of the current trends. This trend has appeared, it has established itself, and is being developed successfully because:

the majority of technical materials are polycrystalline and, therefore, their use in physical investigations provides information directly usable in practical applications;

the structural analysis of polycrystalline samples of some metals has demonstrated convincingly that the majority of grain boundaries in structure-free samples are large-angle boundaries of the general type;

the limitations of the sensitivity of physical research methods, due to the low density of specific states of two-dimensional defects in the bulk of polycrystalline samples, can be reduced somewhat by the use of fine-grained objects.

It should be mentioned however that this trend is naturally limited by the fact that averaging is carried out over an ensemble of grain boundaries in a polycrystalline sample.

Another successfully developing trend involves the use of single exactly characterized grain boundaries in bicrystals. Here, the greatest progress has been made in the Soviet Union and the results are given in Ref. 1. In spite of the

 0038-5670/90/010055-24$01.00

attractiveness of this trend and its high efficacy demonstrated in Ref. 1, there is a natural barrier set by the small size of a grain boundary in a bicrystal. This imposes obvious limitations on the available arsenal of physical methods for the investigation of grain boundaries in bicrystals because of the finite and frequently insufficient sensitivity of these methods.

We shall show later that in some cases it would be possible to utilize simultaneously both bicrystals and polycrystalline samples and it has been found that the properties of these objects are the same, in full agreement with the current ideas on the structure of grain boundaries. Excellent comparisons of the diffusion properties of bicrystalline and polycrystalline samples have been carried out using bicrystals with low-angle tilt boundaries, which consist of rows of edge dislocations.[1] Therefore, in some discussions of the properties of grain boundaries in polycrystalline samples the structure and most general properties of the cores of edge dislocations have been used. However, these clear ideas must not be used beyond the limits of their validity, for example, as the basis for modeling the structure of large-angle grain boundaries of the general type in polycrystalline samples. We shall conclude this section by summarizing briefly the research results and the models and representations based on them.

Major progress has been made recently in the use of atomic probes in the investigation of point defects by nuclear gamma resonance spectroscopy[2] and spectroscopy of perturbed angular correlations.[3] Nuclear gamma resonance spectroscopy has been used also in studies of grain boundaries in metals[4–10] and the main results are presented in Sec. 3. These spectroscopic methods provide direct microscopic information on the states of the atomic probes provided measures are taken to localize the probes near or directly on structure defects. Naturally, it is these trends in physics research that promise the most fruitful approach. The concluding comments summarize the presented material and suggest further research.

1. DIFFUSION PHENOMENA IN REAL CRYSTALS. PREFERENTIAL DIFFUSION ALONG STRUCTURE DEFECTS SUCH AS GRAIN BOUNDARIES

2.1. General relationships governing diffusion in solids

In this section we shall report the most general results of diffusion research and discuss relationships and mechanisms of bulk diffusion in solids which will be used later. Diffusion in solids is due to the presence of point defects. Therefore, diffusion is a unique source of physical data on the point defects responsible for diffusion or on those structure defects in real solids where diffusion is localized (one- and two-dimensional defects, such as dislocations, as well as interfaces including grain boundaries). Diffusion phenomena will be considered later only as a source of physical data on the structure and properties of defects in solids.

When a flux of atomic probes (radioactive or stable tracers) is established in a homogeneous solid, their distribution is described by the relevant Fick laws which contain the diffusion coefficient D acting as the source of physical data. In the general case of heterodiffusion the diffusion coefficient D_2 is given by

$$D_2 = (D_2)_0 \exp\left(-\frac{Q_2}{RT}\right), \tag{1}$$

where

$$(D_2)_0 = a^2 \nu f_2 \exp\frac{S_2}{R}, \tag{2}$$

$$Q_2 = H_2^m + H_2^f - C; \tag{3}$$

here, the index 2 denotes the heterodiffusion parameters. The quantity $(D_2)_0$ is the preexponential factor; Q_2 is the enthalpy of activation; a is the length of a diffusion jump; ν is the "attempt frequency" which is of the same order of magnitude as the frequency of a local mode of vibrations of an atomic probe in the direction of a jump; f_2 is the correlation factor reflecting nonstochasticity of successive jumps of an atomic probe; $S_2 = S_2^m + S_2^f$ is the entropy of activation of diffusion, equal to the sum of entropies of formation and migration of point defects responsible for diffusion; H_2^m and H_2^f are the enthalpy of activation of migration and formation of point defects; $C = -d \ln f_2/d\xi$ is the enthalpy of activation of the correlation factor; $\xi = (RT)^{-1}$; R is the gas constant.

It is clear from Eqs. (1)–(3) that the temperature dependences of the diffusion coefficients can provide information on an important phenomenological parameter which is enthalpy of activation Q_2. A five-frequency model of the vacancy diffusion mechanism gives

$$\frac{D_2}{D_1} = \frac{f_2}{f_1}\frac{\omega_2}{\omega_0}\frac{\omega_4}{\omega_0}\frac{\omega_0}{\omega_3}; \tag{4}$$

where $\omega_i = (\omega_i)_0 \exp(-H)$ are the frequencies of vacancy jumps; ω_2 represents interchange of a vacancy with an atomic probe, ω_1 represents interchange with solvent atoms, still in the vicinity of an atomic probe, and ω_4 and ω_3 represent jumps that result in association and dissociation relative to the atomic probe. The frequencies of elementary jumps defined in this way can be estimated using a microscopic model.

One of the most attractive and fruitful models is the Lazarus–LeClaire vacancy diffusion mechanism.[11,12] An analysis of the difference between the enthalpies of activation of elementary jumps of impurities and host atoms was made in Refs. 11 and 12 allowing for the Coulomb interaction of screened excess charges of point defects participating in an elementary diffusion event. This model was used to show that in the case of impurities with an excess charge (relative to the host) the difference between the enthalpies of activation $Q_{21} = Q_2 - Q_1$ is described by

$$Q_{21} \propto Z_{21} \exp(-qr) - C, \tag{5}$$

where $Z_{21} = Z_2 - Z_1$ is the excess charge of an impurity which in the simplest case is equal to the difference between the valences of the impurity and the host crystals; q is the screening constant; r is the distance from the point charge of the impurity. We shall show later that this approach is fruitful in establishment of the diffusion relationships and mechanisms for metals.

The correlation factor f_2 depends on the same set of frequencies which occurs in Eq. (4):

$$f_2 = \frac{\omega_1 + \omega_3 F}{\omega_2 + \omega_1 + \omega_3 F} = \frac{u}{\omega_2 + u}, \tag{6}$$

so that in general it makes a non-Arrhenius contribution to

the temperature dependence of D_2. In the case of self-diffusion the quantity f_1 is a geometric constant depending on the type of the lattice and diffusion mechanism. Therefore, determination of f_1 is used widely to identify the diffusion mechanism on the basis of the isotopic effect E. It is known[13] that

$$E = \frac{d \ln D}{d \ln m} = f \Delta K, \tag{7}$$

where ΔK is the fraction of the kinetic energy carried by an atomic probe in the direction of a jump. In experimental determination of E it is necessary to find the ratio of the diffusion coefficients to within 0.1%, which can be done only in a few research laboratories even if the latest experimental techniques are used. It was shown in Ref. 14 how the measurements of $D_2(T)$ and $E_2(T)$ can be used to find a set of microscopic parameters representing bulk (volume) diffusion of some impurities.

2.2. Macroscopic description of diffusion phenomena in polycrystalline materials

Preferential grain-boundary diffusion (PGBD) can be made a source of physical information on the structure and properties of grain boundaries provided a correct macroscopic description is used of the diffusion phenomena to be investigated. We shall turn to a clear model of PGBD proposed in Refs. 15 and 16. A polycrystalline sample is represented by a half-space where a plate of thickness d is inserted at right-angles to the surface. The diffusion coefficient within the plate D_{gb} represents the grain boundary, whereas the diffusion coefficient outside the plate represents the bulk of the grain D_{bk}. There is a diffusion source on the surface of this half-space, the distribution of the diffusant concentration in such a system far from this source can be described satisfactorily by the following approximate expression:[15,16]

$$c = c_0 \exp(-\beta y) \operatorname{erfc}\left(\frac{x}{2(D_{bk} t)^{1/2}}\right); \tag{8}$$

here, c_0 is the concentration of atomic probes in the diffusion source; x and y are the coordinates parallel and perpendicular to the surface of the half-space;

$$\beta = \left[\frac{2}{dD_{gb}}\left(\frac{D_{bk}}{\pi t}\right)^{1/2}\right]^{1/2};$$

$$\operatorname{erfc} z = 1 - 2\pi^{-1/2}\int_z^\infty \exp(-u^2)\, du.$$

All the limitations of this approximate description of PGBD by Eq. (8) and its relationship to the exact solutions of the diffusion problem are given in a monograph on the subject.[17] It is important to stress that the inhomogeneity of the diffusion problem is responsible for the two-dimensional nature of the distribution of the concentration in the diffusion zone. In an experimental determination of the quantity dD_{gb} it is usual to employ the values of the concentration in a layer dy perpendicular to the direction of diffusion:

$$\bar{c} = \int_{-\infty}^{\infty} c\, dx = 4c_0\left(\frac{D_{bk} t}{\pi}\right)^{1/2} \exp(-\beta y). \tag{9}$$

We can see that the characteristic feature of the solution (9) is a linear dependence $\ln c(y)$, in contrast to the diffusion in a homogeneous half-space when the linear dependence $\ln c(y^2)$ applies. The exact solutions of the diffusion problem predict the linear dependence $\ln c(y^{6/5})$.

In a mathematical description of PGBD we have to distinguish self-diffusion and heterodiffusion, in contrast to the bulk diffusion. This is due to the changes in the boundary conditions at the grain boundary–grain interface, which govern the behavior of impurity. We have to introduce a coefficient representing the distribution of the impurity between the boundary and the region where the impurity is driven ("pumped"). In the bulk case this coefficient assumes its standard form

$$S = S_0 \exp(E_{ads}\xi). \tag{10}$$

In this case the solutions of the diffusion problem do not contain the combination dD_{gb} for the impurity, but the combination sdD_{gb}. It is assumed that if there are no changes in the structure of the boundary, then the PGBD coefficients, like the bulk diffusion coefficients, depend exponentially on temperature:

$$D_{gb} = (D_{gb})_0 \exp(-Q^*_{gb}\xi). \tag{11}$$

This model of PGBD is quite suitable for the description of the diffusion phenomena in a bicrystal with a planar boundary, but it must be refined in the case of polycrystalline samples. Certain conditions must be satisfied in the experiments in order to ensure that one could use subsequently the clear and simple analytic dependences in describing PGBD in polycrystalline samples.[17,18]

The isotopic effect under the PGBD conditions is described in Refs. 19 and 20 by the following correct approximation:

$$dD_{rp} = \left(\frac{d \ln \bar{c}}{dy^{6/5}}\right)^{-5/3}\left(\frac{4D_{bk}}{t}\right)^{1/2}(0{,}72\beta^{0{,}008})^{5/3}. \tag{12}$$

Hence, we find that

$$\frac{d \ln (c_\alpha/c_\gamma)}{d \ln c_\gamma} = \left[1 - \left(\frac{D_\alpha}{D_\gamma}\right)^{0.286}_{bk}\left(\frac{D_\gamma}{D_\alpha}\right)^{0.592}_{gb}\right]; \tag{13}$$

here, the indices α and γ denote two simultaneously diffusing isotopes. We can see that determination of the ratio $(D_\gamma/D_\alpha)_{gb}$ is even more difficult than in the case of bulk diffusion.

2.3. Experimental results of investigations of relationships governing preferential grain-boundary diffusion in polycrystalline metals

2.3.1. Temperature dependences of preferential grain-boundary diffusion in silver. The use of radioactive or stable tracers, layer-by-layer analysis of a diffusion zone involving measurements of the radiation intensity (or of the relative concentration) in the removed layer, and measurements of the diffusion zone to depths where the concentration of atomic probes decreases by 1.5–2 orders of magnitude from the values at the edge of the PGBD zone are all essential conditions for obtaining PGBD coefficients which are correct and suitable for deriving physical information about these coefficients. Similar requirements apply to the quality of the temperature dependences of the diffusion coefficients. Bearing in mind these conditions, we shall now consider the results obtained in measurements of boundary self-diffusion in silver.[21–27] These investigations were carried out on rolled silver plates recrystallized in 10^{-3} Pa vacuum at 850°C. It

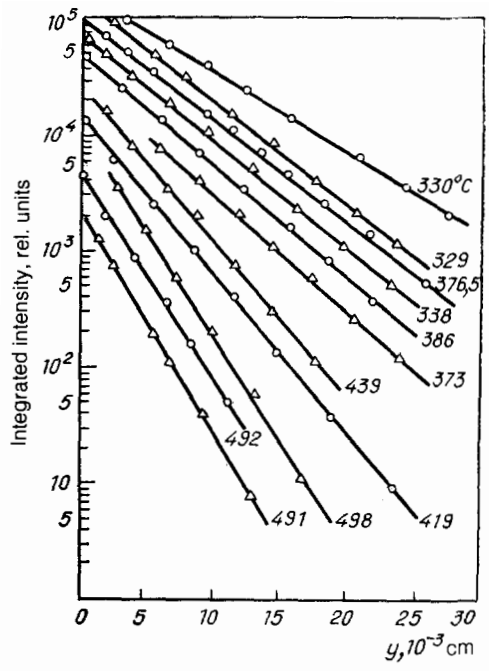

FIG. 1. Coordinate dependences of the concentration of ^{110}Ag in the preferential grain-boundary self-diffusion zone in silver at high temperatures.

was assumed that an ensemble of grain boundaries was a set of large-angle boundaries of the general type.

Figure 1 shows the coordinate dependences obtained for self-diffusion in silver determined in the usual range of temperatures. Clearly, the majority of these coordinate dependences were obtained in the range of relative concentrations amounting to 1.5–3 orders of magnitude. They are all straight lines when plotted as the dependences $\ln c(y)$, which is one of the main criteria confirming the correct selection of the initial and boundary conditions ensuring the validity of the approximate dependences discussed in the preceding subsection.

The autoradiograms recorded for a section perpendicular to the diffusion direction at a depth approximately equal to half the depth of the diffusion zone show that the atomic probes in the form of ^{110m}Ag were indeed localized at grain boundaries in polycrystalline samples and the concentration along the boundaries in this section was approximately the same. Consequently, the hypothesis that large-angle boundaries in such polycrystalline samples were of the same type was well satisfied. Table I gives the parameters of PGBD in the traditional range of temperatures $(0.45–0.65)T_{mp}$. These results are similar to the data on PGBD of gold in polycrystalline silver reported in Ref. 28. Gold is an "isotopic impurity" and should behave in the same way as silver in grain boundaries (Table I). One should mention here two circumstances. Firstly, the ratio of the enthalpies of activation of PGBD Q_{gb} and of the bulk self-diffusion Q_{bk} is 0.35–0.40. The inequality $Q_{gb} < 0.5Q_{bk}$ is not dependent on the bulk diffusion parameters, because the sign of the slope of the dependence $\ln[\alpha_1^2 t^{1/2}(\xi)]$ is governed entirely by the sign of the difference $0.5Q_{bk} - Q_{gb}$. In all the investigations discussed here the value of $d\ln(\alpha_1^2 t^{1/2})/d\xi$ amounts to 2–6.5 kcal/mol, which creates a reliable difference between the values of Q_{gb} and $0.5Q_{bk}$. Secondly, the preexponential factor amounts to 10^{-3} cm^2/s if we accept without question the value $d \approx 5\times10^{-8}$ cm. This preexponential factor is approximately two orders of magnitude less than in the case of bulk diffusion. Turning back to Eq. (2) for the preexponential factor, we can easily see that a difference amounting to two orders of magnitude can be explained in a natural manner by the difference between the entropy terms, which is governed by the frequencies in the vibrational spectrum of those parts

TABLE I.

Impurity	$(D_{bk})_0$, cm^2/s	Q_{bk}, kcal/mol	Q_{21}, kcal/mol	Z_{21}	T, °C	$(\alpha^2 t^{1/2})_0$, cm^{-2}.s$^{1/2}$	$-\frac{d\ln(\alpha^2 t^{1/2})}{d\xi}$, kcal/mol
Au	0.26	45.5±0.9	1.9	−0.2	500÷300		
Ag	0.28	43.4±0.2	0	0	500÷270	$5.1\cdot10^9$	6.5±0,2
					200÷72	$2.8\cdot10^{-3}$	−(7.6±0,4)
Cd	0.50	42.2±0.2	−1.2	1	500÷280	$2.4\cdot10^9$	5.7±0,3
In	0.55	41.8±0.5	−1.6	2	490÷260	$2.1\cdot10^9$	5.3±0,2
					180÷100	$6\cdot10^3$	−(6.3±0,5)
Sn	0.47	40.8±0.1	−2.6	3	500÷280	$1.3\cdot10^9$	6.1±0,2
					160÷100	$4.1\cdot10^2$	−(8.1±1,7)
Sb	0.27	39.4±0.3	−4.0	4	500→280	$0.8\cdot10^9$	5.9±0,2
					180÷100	$6.8\cdot10^2$	−(9.0±0,7)
Fe	0.21	36.9±0.2	−6.5	5	700÷350		8.5±0,3
					300÷156		−(10.5±0.5)

Impurity	$(sdD_{gb})_0 \times 10^{10}$, cm^3/s	Q^*_{gb}, kcal/mol	Q_{segr}, kcal/mol	Q_{gb}, kcal/mol	$(D_{gb})_0$, cm^2/s	$(D_{disl})_0 \times 10^7$, cm^2/s	Q_{disl}, kcal/mol	Q^{LT}, kcal/mol
Au	20	18.0						
Ag	1.2	15.2±0.4	0	15.2	3			26.6
						1	15.2	26.6
Cd	3.3	15.4±0.4	1.5	17	8			
In	3.9	15.2±0.4	−2.5	18	9.5			
						60	13.0	27.5
Sn	6	14.3±0.2	−4	18	15			
						0.6	16.0	27.4
Sb	7.3	13.8±0.3	−6	20	18			
						2.5	18.0	27.6
Fe	17	10.1±0.3	−11	21	41			
							20.0	29.0

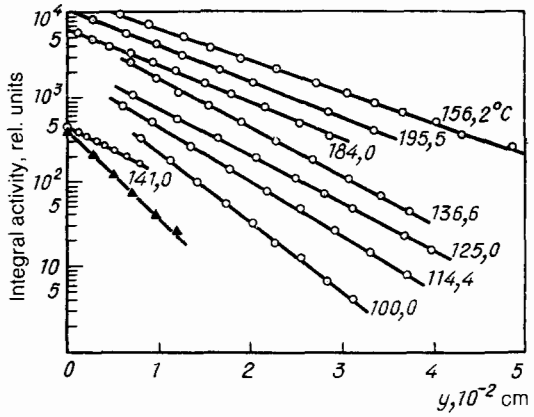

FIG. 2. Coordinate dependences of the concentration of ^{110}Ag in the preferential grain-boundary self-diffusion zone in silver at low temperatures.

of a crystal where the diffusion takes place. Consequently, there are good reasons for the conclusion that the entropy of activation of grain-boundary diffusion is considerably less than the corresponding entropy of bulk diffusion, i.e., the frequencies of vibrations in grain boundaries are lower than in the bulk. This conclusion will be checked later in a discussion of the properties of impurity states in grain boundaries.

The quality of the temperature dependences of the grain-boundary self-diffusion coefficients of polycrystalline silver was improved in an investigation reported in Ref. 21 by extending greatly (in the direction of lower temperatures) the temperature range in which PGBD was investigated. It should be pointed out that the nature of the distribution of the concentration of ^{110m}Ag in the diffusion zone remained unchanged at low temperatures (Fig. 2), indicating that the diffusion fluxes typical of PGBD remained two-dimensional. However, the PGBD parameters calculated from these temperature dependences behaved in a completely unexpected manner. This can be seen from Fig. 3, which gives the dependence $\ln[\alpha^2 t^{1/2}(\xi)]$ for the whole temperature range under investigation. Clearly, the enthalpies of activation of diffusion fluxes, governing self-diffusion in the PGBD zone, began to change at $T = 0.45T_{mp}$ and gave rise to a new stable Arrhenius dependence of the PGBD parameters beginning from $T = 0.3T_{mp}$, where T_{mp} is the melting point of the host crystal.

In order to stress the universality of the effect discovered by the present author and not predicted earlier, we should mention that it is typical of all the PGBD impurities investigated in silver, including the recent unique results obtained by implantation of radioactive atomic probes.[29] Moreover, the effect was also found recently in a study of PGBD in other f.c.c. metals. Therefore, identification of the physical origin of the effect is of fairly general importance.

The kink in the Arrhenius dependence $\ln[\alpha^2 t^{1/2}(\xi)]$ is unrelated to any other assumptions, apart from the macroscopic description of diffusion fluxes in an inhomogeneous sample. It is traditionally assumed that two-dimensional diffusion fluxes are governed by fast diffusion along grain boundaries and "pumping out" of the diffusant from the boundaries and transfer to the adjoining regions of the regular lattice by *bulk* diffusion throughout the *investigated temperature range*. This hypothesis is based on retention of the linear dependences $\ln C(y)$ at all the investigated temperatures. In fact, using the parameters of the bulk self-diffusion in silver (Table I), we can easily show that the criterion[17]

$$20(D_{bk}t)^{1/2} < d \tag{14}$$

of transition to a one-dimensional diffusion flux in the PGBD zone begins to be satisfied already at temperatures of about $0.38T_{mp}$ (approximately 200°C). Consequently, a major part of the "new" Arrhenius dependence is related to a different mechanism of formation of a two-dimensional flux in the PGBD zone, i.e., to a different mechanism of "pumping out" of the diffusing substance from the actual grain boundary. Two new mechanisms of such "pumping out" are possible and these begin to act only when the bulk "pumping out" is frozen:

when the front of the diffusion flux of atomic probes from grain boundaries is localized in the region of a layer of adsorption accumulation near the boundary, the properties of this layer begin to determine the characteristics of the "pumping" process, but the absence of any reliable data on the diffusion properties of an adsorption accumulation layer in silver means that this mechanism cannot be used to judge the experimental results;

when the number of atomic probes in the bulk "pumping out" zone is sufficiently small and comparable with the number of these probes in the grain boundary itself, the "pumping out" kinetics may be affected by a flux of atomic

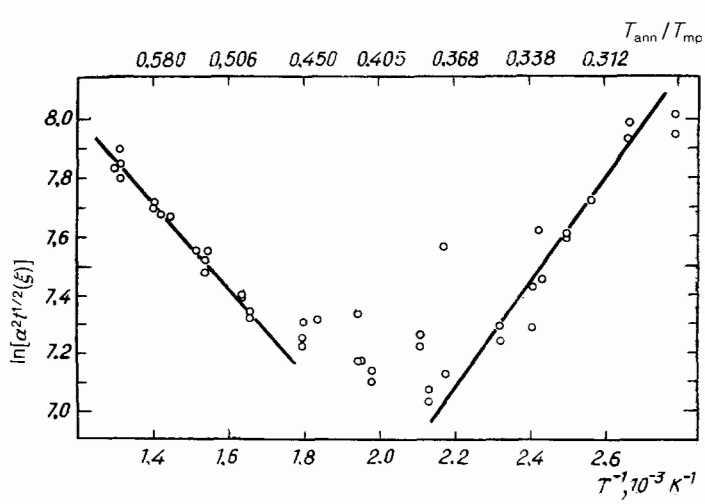

FIG. 3. Temperature dependences of $\ln[\alpha^2 t^{1/2}(\xi)]$ for preferential grain-boundary self-diffusion in silver.

probes between lattice dislocations, which intersect the grain boundary. The description of grain-boundary diffusion with a dislocation "pump" is formulated in Ref. 21. In the range of temperatures where this dislocation mechanism predominates, we find that subject to some natural assumptions, we obtain

$$\alpha_2^2 t^{1/2} = 2(m r_0^2 D_{\rm disl})^{1/2}(dD_{\rm gb})^{-1}, \qquad (15)$$

where $\alpha_2 = \mathrm{d}\ln C/\mathrm{d}y$ is the slope of the coordinate dependence at low temperatures; m is the density of lattice dislocations intersecting the grain boundary; r_0 is the effective radius of a dislocation, $D_{\rm disl}$ and $D_{\rm gb}$ are the coefficients of the dislocation and grain-boundary diffusion mechanisms, respectively. We can see that the coefficient $D_{\rm disl}$ occurs in the same combination as the bulk diffusion coefficient $D_{\rm bk}$ in Eq. (9) describing α_1. Hence, the enthalpy of activation is described by

$$-\frac{d\ln(\alpha_2^2 t^{1/2})}{d\xi} = \frac{Q_{\rm disl}}{2} - Q_{\rm gb}. \qquad (16)$$

Since $0.5Q_{\rm disl} < Q_{\rm gb}$, it follows that the slope of the dependence $\ln[\alpha^2 t^{1/2}(\xi)]$ in the dislocation "pump" region changes sign compared with the slope in the bulk "pump" region, as is indeed observed.

Table I lists the parameters of three diffusion fluxes encountered in polycrystalline silver. We can see that the enthalpies of activation of the grain-boundary and dislocation diffusion processes are equal. This important result demonstrates that the paths of accelerated diffusion in grain boundaries and in lattice dislocations are identical. This is in excellent agreement with the dislocation-models of the structure of grain boundaries in metals.[30]

We shall now present the results of an investigation of the relationships governing grain-boundary diffusion of impurities in silver. As pointed out in the Introduction, the use of atomic probes in the form of impurities differing from the solvent only in respect of the excess charge has made it possible to describe quantitatively the systems based on silver using the model of vacancy diffusion mechanisms, which then accounts for all the diffusion effects in such systems. Hence, it seems justified to use a similar approach in the studies of diffusion phenomena in grain boundaries in order to identify the atomic mechanism of diffusion in these boundaries.

Figure 4 shows typical temperature dependences of the diffusion permeability of grain boundaries in silver $sdD_{\rm gb}$ for various impurities. Clearly, if we continue to use the arbitrary representation of the bulk "pumping out" from grain boundaries, then the kink appears in approximately the same temperature interval for all the impurities belonging to the same row as Ag in the periodic table. It should be stressed that the temperature dependence of $sdD_{\rm gb}$ in the case of tellurium was obtained independently by a research team working in Münster.[29] In interpretation of the results on PGBD of impurities we must allow for the temperature dependence of segregation of impurities at grain boundaries. Estimates of $E_{\rm ads}$ have been reported for these systems.[31] Using the estimates obtained there, we can find the values of $Q_{\rm gb}$ for PGBD of impurities. Figure 5 shows the dependences of the differences $(Q_{\rm gb})_{21}$ between the enthalpies of activation of heterodiffusion $(Q_{\rm gb})_2$ and self-diffusion $(Q_{\rm gb})_1$ on the excess charges Z_{21} carried by impurities from the same row in the periodic table as Ag. We can see that an increase in Z_{21} increases also $(Q_{\rm gb})_{21}$, contrary to the vacancy mechanism of bulk diffusion in silver (Fig. 5). The *opposite signs* of these dependences clearly indicate that the mechanisms of diffusion in the regular lattice and along the accelerated diffusion paths in grain boundaries are different. The dislocation enthalpy of activation behaves similarly to $(Q_{\rm gb})_{21}$ and this confirms the correctness of our estimates of the enthalpies of segregation of impurities of the Ag row in the periodic table on grain boundaries in silver. Finally, using the relationships between the enthalpy and entropy of activation of diffusion, well tested empirically and by model representations,[32,33] we find that

$$S \propto \frac{H^{\rm m}}{T_{\rm пл}}, \qquad (17)$$

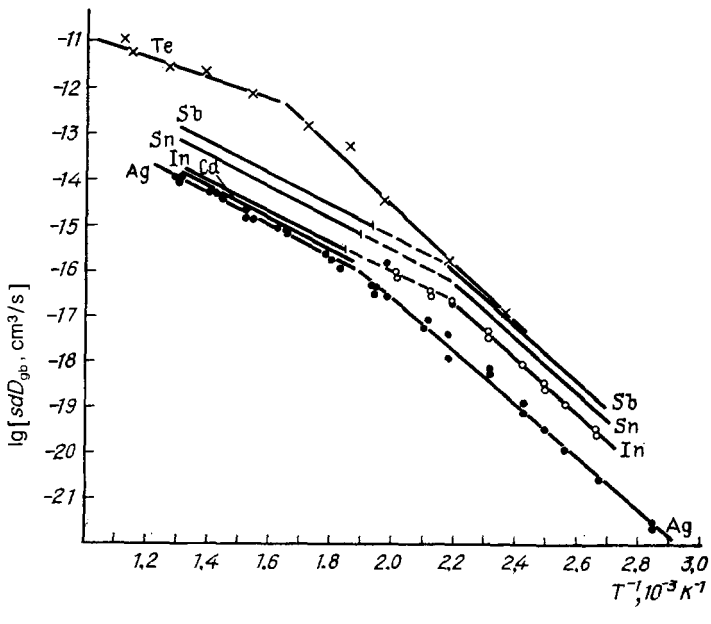

FIG. 4. Temperature dependences of $\lg[sdD_{\rm gb}(\xi)]$ for preferential grain-boundary diffusion in silver.

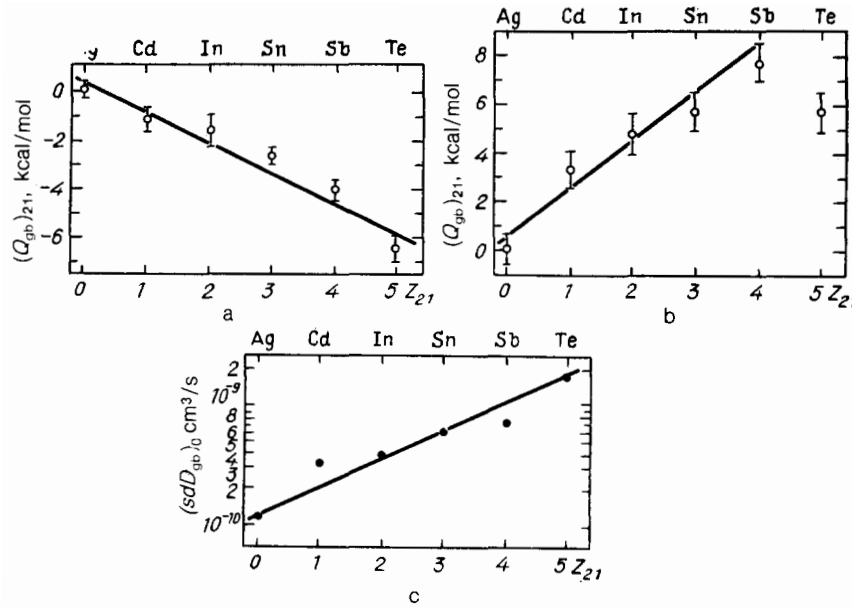

FIG. 5. Dependences of the parameters of bulk and preferential grain-boundary diffusion of impurities in silver on their excess charge.

where S and H are the entropy and enthalpy of diffusion, respectively. It therefore follows that

$$\ln D_0 \propto S \propto H. \tag{18}$$

Consequently, the nature of the changes in $\ln D_0$ in the case of this row of impurities should be identical with the dependence of the enthalpy of activation on their excess charge. Figure 5 shows the dependence of $\lg(D_{gb})_0$ on Z_{21}, which obviously confirms fully the above conclusions on qualitative differences between the charge dependences of the enthalpies of activation of grain-boundary and bulk diffusion.

Which diffusion mechanism does not contradict the relationships described above? Obviously, all the characteristics of PGBD discovered so far can be described most fully on the basis of model representations of interstitial diffusion in grain boundaries. It is known that the low enthalpy of activation, representing approximately half of the enthalpy of activation of bulk self-diffusion, is the distinguishing feature of the interstitial diffusion mechanism. It is due to the absence of the enthalpy of formation of a defect, responsible for the elementary jumps of an atom. Another characteristic feature of this diffusion mechanism[34] is the positive sign of the derivative dQ_{21}/dZ_{21}, which is in full agreement with the relationship found by us for PGBD of impurities belonging to the same row in the periodic table as silver. Finally, in the case of the interstitial diffusion mechanism there are two very different values of the correlation factor: $f_2 = 1$ for interstitial atoms localized fully at lattice interstices and $f_2 = 0.40$–0.44 for split interstitials, which appear when an interstice captures a host ion.[35] Using the available data, we can see that the interstitial mechanism accounts completely for all these relationships and that the vacancy mechanism fails to explain most of them.

2.3.2. Temperature dependences of preferential grain-boundary diffusion in other f.c.c. metals (copper and nickel). The experimental techniques described in the preceding subsections were used also to investigate PGBD of impurities in copper of the copper row elements in the periodic table.[36–42] Autoradiograms of sections of the diffusion zone and the coordinate dependences of the concentration of the atomic probe indicated that the solutions of the diffusion problem were satisfied rigorously by the results which were analyzed. Although in the case of these systems only the traditional temperature range $T > 0.46T_{mp}$ was investigated, the results demonstrated clearly that once again the main relationships established for silver were obeyed. In fact, the quantity $\lg(D_{gb})_0$ rose rapidly on increase in Z_{21}, which indicated that $d(Q_{gb})_{21}/dZ_{21} > 0$. The use of estimates of elastic en-

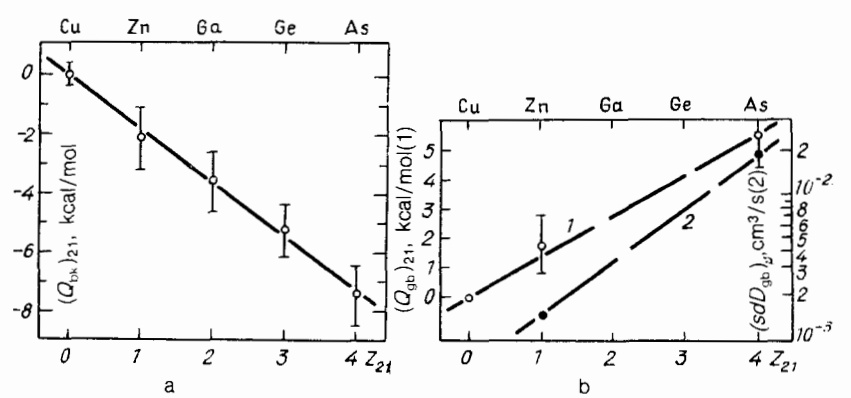

FIG. 6. Dependences of the parameters of the bulk and preferential grain-boundary diffusion of impurities in copper on their excess charge.

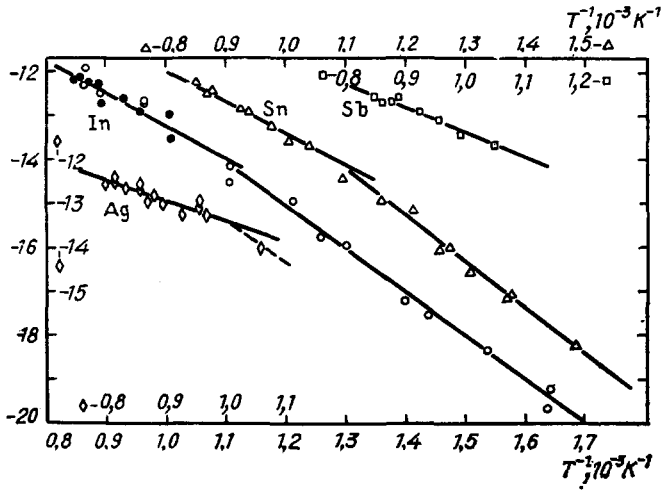

FIG. 7. Temperature dependences of $\lg[sdD_{gb}(\xi)]$ for preferential grain-boundary diffusion in nickel.

thalpies of the segregation of impurities of the copper row in the periodic table gave results presented in Fig. 6. This figure gives the dependence of $(Q_{bk})_{21}$ on the excess charges of impurities belonging to the copper series and it demonstrates that in the case of bulk diffusion in copper the consequences of the vacancy diffusion mechanism can be seen. A comparison with the dependences for PGBD demonstrate a qualitative difference between the atomic diffusion mechanisms in the bulk and in grain boundaries in copper.

The experimental results of an investigation of the grain-boundary self- and heterodiffusion in nickel can be divided in a natural manner into two groups. The first consists of the results reported in Refs. 43–44 in the traditional high-temperature range: $(0.5–0.7)T_{mp}$. The second represents the recent results obtained in a much wider temperature range: $(0.35–0.7)T_{mp}$. The investigations which yielded the second batch of results are carried out using the latest techniques for experimental studies of diffusion.[31,45,46] We shall not give more typical coordinate dependences but simply note that in the case of investigations of the second group all the dependences were linear when plotted using the coordinates $\ln C(y^{6/5},)$ indicating that the two-dimensional nature of the diffusion flux was retained in polycrystalline and bicrystalline samples of nickel even when $(D_{bk}t^{1/2}) \approx (0.3–20) \times 10^{-8}$ cm. Consequently, as in the case of polycrystalline silver, at the lowest temperatures used in the investigations of nickel the bulk "pumping out" disappeared in the case of PGBD and the characteristic two-dimensional nature of the diffusion flux was retained.

Figure 7 gives the temperature dependences of PGBD

TABLE II.

Impurity	Z_{21}	$(D_{bk})_0$, cm²/s	Q_{bk}, kcal/mol	Q_{21}	T, °C	$(sdD_{gb})_0$, cm³/s
Ni	0	1.8	68.1±0.1	0	1100÷550 1000÷350	$4\cdot10^{-9}$ $4\cdot10^{-5}$
Ag	0.5	8.9	66.7±0.6	−1.4	980±760	$1.3\cdot10^{-9}$
In	2.0	6.8	64.6±0.4	−3.5	910÷730 635÷336	$8.6\cdot10^{-7}$ $5.1\cdot10^{-4}$
Sn	2.7	4.6	63.8±0.2	−4.3	900÷680 640÷400	$3.6\cdot10^{-7}$ $1.6\cdot10^{-3}$
Sb	2.7	3.8	63.1±0.2	−5.0	900÷680 1000÷300	$1.0\cdot10^{-8}$ $1.1\cdot10^{-5}$
Te		2.6	61.0±0.2	−7.1	700÷270	$2.2\cdot10^{-11}$

Impurity	Q^*_{gb}, kcal/mol	Q_{segr}, kcal/mol	Q_{gb}	$(D_{gb})_0 \times 10^9$ cm²/s	Q_{disl}, kcal/mol
Ni	27.4±0.8 44.7±0.5	0	27.4	1.1	21.5
Ag	21.0±2.5	−1.0	22	0.37	
In	32.7±1.5 44.6±0.5	−5.0	38	2.5	25
Sn	31.5±1.0 47.3±0.5	−6.0	37.5	100	31
Sb	24.1±2.0 40.1±0.5	−9.0	33	2.8	19
Te	38.2±0.5	−11.0			15

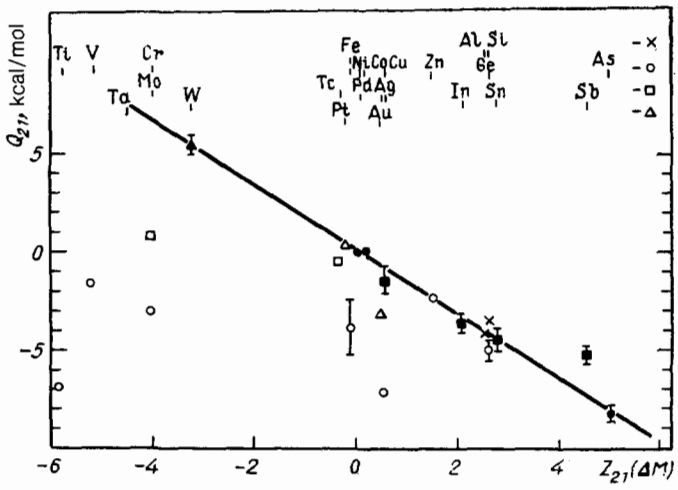

FIG. 8. Dependence of the enthalpies of activation of bulk diffusion on the excess charge of impurities in nickel.

of impurities in nickel. In all cases, when the investigated temperature range was sufficiently wide, there was a kink in the temperature dependences of the PGBD coefficients. The position of this kink T_{kink} (Ni) = (0.50–0.53) T_{mp} practically coincided with the position of the kink on the scale of homologous temperatures for the PGBD coefficients of migration in silver: T_{kink} (Ag) = (0.45–0.48) T_{mp}. The parameters of PGBD of impurities in nickel are listed in Table II. Before discussing the data on PGBD of impurities in nickel, we shall first consider the results of investigations of bulk diffusion in this metal.

Figure 8 gives the enthalpies of activation of bulk diffusion of impurities in nickel as a function of the excess charges of impurities.[47] In the case of silver and copper the definition of the excess charges of impurities belonging to the same rows in the periodic table (sp impurities) can naturally be defined as the difference between the valences, which is quite justified and usual, whereas the situation in nickel is greatly complicated by the redistribution of the excess charge between the s and d electron energy bands of the host crystal and by the possibility of formation of bound states at the impurity sites. A detailed theoretical analysis of the state of impurities representing elements belonging to the 3d and 4d periods migrating in nickel[48] has shown that it is possible to use the simple and clear results of the rigid band model to calculate the excess charges of impurities in nickel from the saturation magnetization of the relevant solid solutions.

We can see from Fig. 8 that in the case of many transition impurities and for practically all the sp impurities it is possible to establish the relationship between the enthalpy of heterodiffusion and the correctly defined excess charges. In addition to the correct determination of the quantity Z_{21}, a decisive role in establishing this dependence is played by the qualitative results obtained for high-purity nickel single crystals investigated by the modern experimental techniques for the investigation of diffusion.

Figure 9 shows the dependence of the enthalpy of activation of PGBD in nickel plotted on the basis of Table II. Even low values of Q^*_{gb} describing the gently sloping high-temperature parts of the temperature dependences of the PGBD coefficients in nickel are scattered in an irregular manner in a wide band of values. An approximately the same situation applies also to the enthalpies of activation describing the steep low-temperature parts of these dependences. Therefore, it is hardly meaningful to try to find relationships on the basis of the existing experimental data on PGBD in nickel. In view of the great practical importance of the relationships governing grain-boundary diffusion in nickel, it would be highly desirable to carry out systematic investigations governing these relationships in the case of PGBD in nickel using modern diffusion experimental techniques.

In view of the obvious difficulties the use of gold as the host in diffusion studies has been very rare. We shall not consider the relationships governing the processes of bulk diffusion of impurities in gold, which are on the whole in agreement with the detailed investigations of the systems based on silver and copper, but concentrate on preferential grain-boundary self-diffusion carried out in a wide range of temperatures and reported only in Refs. 49–51. Table III gives the parameters of the bulk, grain-boundary, and dislocation self-diffusion of gold and heterodiffusion of silver[52] in gold. It should be stressed that the low-temperature data reported in Ref. 51 were not obtained for bulk polycrystalline samples with recrystallized boundaries, but for thin films which were evaporated either on magnesium oxide or on quartz covered by a molybdenum barrier layer. The absence of monitoring of the composition of these films after diffusion annealing has failed to exclude the possibility of their doping during deposition and during annealing. More-

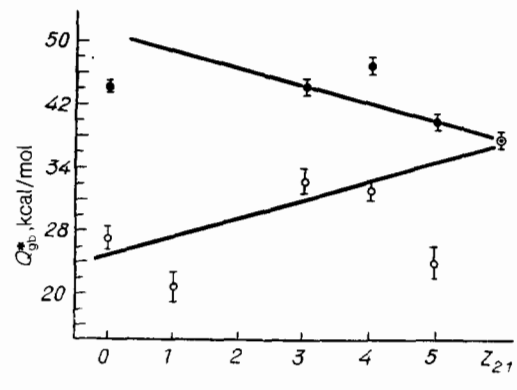

FIG. 9. Dependences of the parameters of preferential grain-boundary diffusion of impurities in nickel on Z_{21}.

TABLE III.

Impurity	$(D_{bk})_0$, cm²/s	Q_{bk}, kcal/mol	Q_{Zt}	T, °C	$(sdD_{gb})_0 \times 10^{10}$ cm³/s	Q^*_{gb}, kcal/mol	T, °C	$(r^2D_{dis})_0$, cm³/s	Q_{dis}, kcal/mol
^{195}Au	0.04	41.4±0.05	0	367—444	3.1	20.3±0.5	247—352	$2\cdot10^{-10}$	26.7±0,5
				117—177	9	23.0±2.3			
^{110}Ag	$8.6\cdot10^{-2}$	40.4±0.2	−1.0	30—260	$5\cdot10^{-3}$	14.5			
				150—260	$5\cdot10^{-4}$	25.3			
				275—536	9,5	16.2±0.8			

over, the ensemble of recrystallized grain boundaries in a bulk polycrystalline sample may be different from that in a thin film, as indicated by much direct experimental evidence.

2.3.3. Temperature dependences of coefficients representing preferential grain-boundary diffusion in tungsten. Investigations of the relationships governing PGBD in polycrystalline samples of refractory metals have not been carried out until very recently for two important reasons: melted polycrystalline samples of refractory metals have not been sufficiently pure and the deformation followed by recrystallization of the initially pure single crystals are very difficult to achieve because of the tendency of these materials to crack at high degrees of cold deformation. Therefore, the relevant investigations, clearly of considerable interest, have been carried out only very recently.

The classical layer-by-layer analysis of the diffusion zones was used in Ref. 53 to investigate PGBD of ^{57}Co in remelted polycrystalline tungsten with the nominal purity grade 3N8. High-temperature annealing in 10^{-6} Pa vacuum stabilized the grain size at 150 μm. The use of ^{57}Co without a carrier guaranteed that the results were free of the influence of the very low solubility of cobalt in tungsten and of the effects of the composition dependences of the investigated PGBD parameters.

By way of example, Fig. 10 shows the coordinate dependences of the cobalt concentration in tungsten illustrating PGBD of ^{57}Co and the high resolution and sensitivity of the classical layer-by-layer analysis. Clearly, at the lowest temperature of the diffusion annealing amounting to 963 K the distribution of the concentration in the diffusion zone was exactly that expected for a two-dimensional diffusion flux in the region of the grain boundaries, although the effective depth of bulk diffusion at this temperature given in Ref. 53, is only $(D_{bk}t)^{1/2} \approx 5\times10^{-9}$ cm. There are, however, grounds for assuming that the correct value is $(D_{bk}t)^{1/2} \approx 4\times10^{-12}$ cm. This is another and very striking piece of evidence of the important circumstance mentioned in the preceding subsections that at low temperatures when the bulk "pumping out" from grain boundaries is completely frozen out, the nature of the distribution of the impurity concentration in the PGBD zone remains the same as at high temperatures. The very low values of $(D_{bk}t)^{1/2}$ can be obtained only for refractive metals such as tungsten, which makes these metals important model materials for the investigation of the physical relationships governing PGBD.

Figure 11 gives the temperature dependence of the diffusion permeability of grain boundaries in tungsten. We can see that, in contrast to the earlier data mentioned above, this dependence exhibits a double kink. The first is located at $0.4T_{mp}$, which is exactly the same homologous temperature as in the case of silver and nickel. At this temperature the effective depth of the bulk "pumping-out" is $(D_{bk}t)^{1/2} = 2\times10^{-8}$ cm. The second kink, observed for the first time, is located at the homologous temperature of $0.35T_{mp}$ reached also in other systems based on silver and nickel, but not identified for these systems because of the special nature

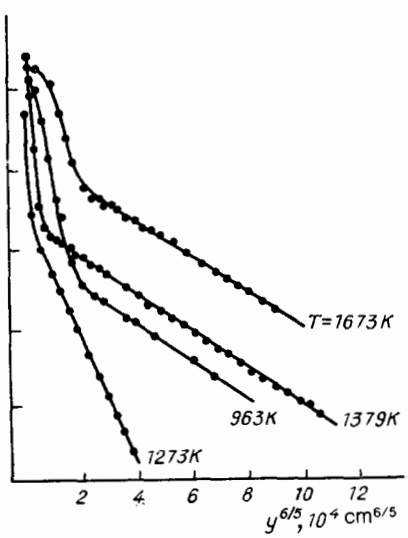

FIG. 10. Coordinate dependences of the concentration of ^{57}Co in the preferential grain-boundary diffusion in *W*.

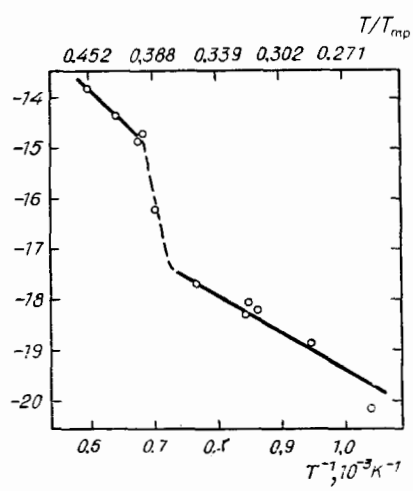

FIG. 11. Temperature dependence of $\lg[sdD_{gb}(\xi)]$ for preferential grain-boundary diffusion of ^{57}Co in *W*.

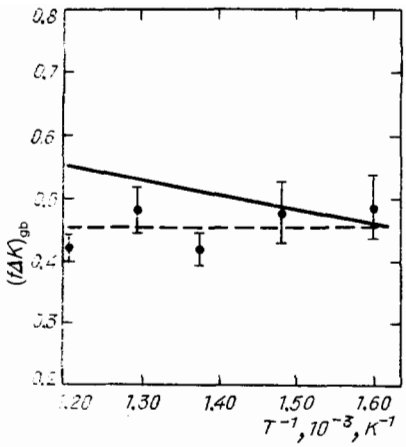

FIG. 12. Temperature dependence of $E_{gb}(\xi)$ for preferential grain-boundary selfdiffusion in silver.

of the temperature dependences of the PGBD parameters.

2.3.4. Isotopic effect in preferential grain-boundary self-diffusion in silver. It has already been pointed out in Sec. 2.2 that measurements of the isotopic effect in the course of diffusion present serious experimental difficulties because of the need to determine the ratio of the diffusion coefficients of two isotopes to within 0.1%. In the case of the isotopic effect during PGBD the difficulties are enhanced proportionally to reduction in the concentration of the radioactive tracers in the PGBD zone (by two or three orders of magnitude) compared with the analogous conditions in the bulk diffusion zone, which is due to a corresponding increase in the difficulties of ensuring the necessary statistical precision of measurements of the ratios of concentrations of two simultaneously diffusing isotopes. The results of unique measurements of the isotopic effect in the course of grain-boundary self-diffusion in silver polycrystalline and bicrystalline samples of different orientations are reported in Ref. 20. Figure 12 and Table IV give the temperature dependence of the quantity $E_{gb} = (f_1\Delta K)_{gb}$. We can see that, within the range of a fairly considerable scatter, the enthalpy of activation $C = -\mathrm{d}\ \ln(E/\Delta K)/\mathrm{d}\xi$ is zero. Information on the PGBD mechanism can be obtained from the isotopic effect under PGBD conditions if:

the value of ΔK_{gb} and its possible temperature dependence are estimated or reasonable assumptions are made about them;

theoretical calculations of the correlation factor are available for different PGBD mechanisms, which can be compared with the experimental results.

Unfortunately, at present these two requirements are strictly speaking unsatisfied. True, the authors of Ref. 19 calculated the correlation effects for the vacancy diffusion mechanism along grain boundaries assuming the boundary has a special plane on which the concentration of the segregated vacancies is maximal, thus implying that the main factor which must be allowed for above others is the change in the concentration of vacancies in the plane of the boundary as a result of a reduction in the energy formation of vacancies related to the binding energy of vacancies and the boundary (Table IV). A correct calculation of the correlation effects in self-diffusion along dislocations of different types was made in Ref. 54 for the vacancy diffusion mechanism.

However, as demonstrated in the preceding sections, the relationships governing grain-boundary heterodiffusion support the nonvacancy mechanism and this is clearly the interstitial mechanism. If we assume the interstitial mechanism in the explanation of the isotopic effect in the course of PGBD, we find that the results obtained by the authors cited above can be explained in a simple and natural manner. First of all, it is well known that host interstitials cannot exist in the bulk of a crystal in the form of isolated atoms at interstices. They in fact form dumbbell configurations which have a number of unique properties. In particular, the correlation factor for a "split" host interstitial in the fcc lattice is 0.45 instead of 1 for a single atom at an interstice. We can clearly assume that in the case of diffusion of such split interstitials in the core of a grain-boundary dislocation the correlation factor is considerably less than a single interstitial atom in the same region. Naturally, then E_{gb} is considerably less than E_{bk}, because it follows from the theory that the correlation factors of the dumbbell, vacancy, and interstitial configurations are related by

$$f_{\mathrm{dumb}} < f_{\mathrm{vac}} < 1 = f_{\mathrm{interst}}. \tag{19}$$

Secondly, for any variant of the interstitial diffusion mechanism there is only one natural jump frequency, which ensures that the correlation effects of this mechanism are independent of temperature.

Therefore, one of the most sensitive tests of the diffusion mechanism, which is the isotopic effect during diffusion, can be explained on the qualitative level equally satisfactorily as mechanisms of interstitial and vacancy diffusion in the cores of grain-boundary dislocations.

2.4. Conclusions

The use of the atomic probe method in investigations of the relationships governing diffusion phenomena in grain

TABLE IV.

Sample	T, °C	$1-(D_{110}/D_{105})_{gb}$	$(f\Delta K)_{gb}$	f (H^B =2300 kcal/mol
Polycrystalline sample	350.0	0.011±0.001	0.49±0.05	
	400.6	0.011±0.001	0.47±0.08	0.56
	453.3	0.010±0.000	0.42±0.03	
	498.1	0.011±0.001	0.49±0.03	0.62
	555.5	0.010±0.000	0.42±0.02	0.67
[100]	400.6	0.010±0.002	0.43±0.10	
	498.1	0.012±0.001	0.52±0.06	
Single crystal	640.0	0.016±0.000	0.70±0.01	

Here, [100] is the axis of rotation of crystallites in a bicrystal

boundaries of the recrystallization type in metals has established that:

the temperature dependence of the diffusion permeability of grain boundaries in metals exhibits a kink at temperatures of the order of $(0.40–0.45)T_{mp}$;

at high temperatures, when the "clinical picture" of PGBD is governed by two fluxes—along a grain boundary and out of the grain boundary into the bulk—we have

$$Q_{gb} = (0.3 - 0.4)Q_{bk}, \tag{20}$$

which is evidence of a basically new (different from the vacancy mechanism of diffusion in a regular lattice) diffusion in the cores of structure defects such as dislocations and grain boundaries;

the high-temperature grain-boundary diffusion coefficients are given by

$$(D_{gb})_0 = 10^{-3}\ \mathrm{cm^2/s} = (10^{-3}–10^{-2})(D_{bk})_0, \tag{21}$$

which is due to the low entropy of activation of PGBD, reflecting the "softening" of the spectrum of the local vibrations of atomic probes within the grain-boundary region compared with a regular lattice;

in the case of preferential grain-boundary heterodiffusion the enthalpy of activation Q_{gb} increases [like the preexponential factor (D_{gb})] on increase in the excess charge of the impurity Z_{21}: $d(Q_{gb})_{21}/dZ_{21} > 0$, in contrast to the analogous dependence in the case of the vacancy diffusion mechanism which is characterized by $d(Q_{bk})_{21}/dZ_{21} < 0$. This is evidence of the interstitial diffusion mechanism within grain boundaries;

the combination of the interstitial positions of atomic probes within a grain boundary with a softened spectrum of local vibrations is a characteristic criterion of the presence of split interstitials, containing an atomic probe diffusing within a grain boundary;

at low temperatures when the diffusion flux remains two-dimensional in a polycrystalline sample, the "pumping out" from a grain boundary does not disappear even when $(D_{pump}t)^{1/2} \ll 10^{-8}$ cm, which is evidence of a new mechanism of "pumping out" at these low temperatures;

at low temperatures the process of preferential grain-boundary self-diffusion is governed by

$$Q_{pump} = Q_{gb} \text{ and } (D_{pump})_0 = (10^{-4} - 10^{-3})(D_{gb})_0, \tag{22}$$

which provides the basis for developing a model of dislocation "pumping out," but this does not exclude the participation of a layer of adsorption accumulation of impurities and vacancies near a grain boundary and formation of a low-temperature "pump" acting on atomic probes.

3. NUCLEAR GAMMA RESONANCE SPECTROSCOPY OF IMPURITY STATES AT GRAIN BOUNDARIES

3.1. Clinical picture provided by nuclear gamma resonance spectroscopy for polycrystalline samples of metals

As pointed out in the Introduction, the use of atomic probes provides, in principle, an opportunity for obtaining *direct microscopic information* on electronic and dynamic properties of solids and on the structure of defects. This opportunity can be utilized in the case of states at grain boundaries by ensuring effective localization of atomic probes within the *cores* of grain boundaries.

It is natural to use the phenomenon of preferential grain-boundary diffusion (PGBD) to deliver atomic probes along accelerated diffusion paths to positions about which we need microscopic information. The results of the representations given above can be used to predict qualitatively the patterns of nuclear gamma resonance (Mössbauer) spectra which can be expected for a polycrystalline sample after it is diffusion-saturated at low temperatures by an impurity capable of nuclear gamma resonance, such as ^{57}Co.

If the diffusion annealing is carried out at PGBD temperatures such that the number of atomic probes in the core of a grain boundary is comparable with their number in the "pumping out" region near the boundary, the nuclear gamma resonance spectrum should include:

a component due to states located in the "pumping out" zone;

one or more components due to the states in the cores of grain boundaries which can be reached by a diffusing atomic probe.

On the basis of the results in Sec. 2 we can expect a change in the temperature and duration of diffusion annealing to alter also the relationships governing the populations of the states under consideration (because of the different enthalpies of activation and diffusion coefficients of atomic probes the relevant positions) and, consequently, there should be a change in the ratio of the intensities between these two types of nuclear gamma resonance (NGR) lines. For example, the NGR line due to the states in the "pumping out" zone (L_1 line) should be the only line in the NGR spectrum of a polycrystalline sample as long as the number of occupied states in the "pumping out" zone is much greater than the number of occupied states within the grain boundary itself. This is due to the linear scale of the intensities in NGR spectroscopy, which makes it possible to detect reliably the components of intensities amounting to just a few percent of the intensity of the main component or components. At these high temperatures ($T > 0.45T_{mp}$) it is possible to obtain information on the states of atomic probes located within the zone representing high-temperature bulk diffusion "pumping out."

Reduction of the temperatures of the diffusion saturation of polycrystalline samples with atomic probes in the range $0.35T_{mp} < T < 0.45T_{mp}$ can make the number of these probes in the "pumping out" zone comparable with their number in a grain boundary, so that an NGR spectrum may exhibit new components in the form of L_{2i} lines. Lowering of temperature in this "range of observation" of the states in grain boundaries should reduce the intensity of the L_1 component (reducing the relative population of the "pumping out" states because of the lower diffusion coefficients and the higher enthalpy of activation of the "pumping out" in this range of temperatures).

Finally, at still lower temperatures the diffusion annealing, where—as shown in Sec. 2—there is a change in the mechanism of "pumping out" from grain boundaries, there should be a further change in the relationships describing the level populations and reflecting the macroscopically observed characteristics of PGBD.

We shall now turn to the experimental results reported in Refs. 4–10. Figures 13 and 14 show the NGR spectra obtained for palladium and tungsten at room temperature using a potassium ferrocyanide absorber enriched with ^{57}Fe

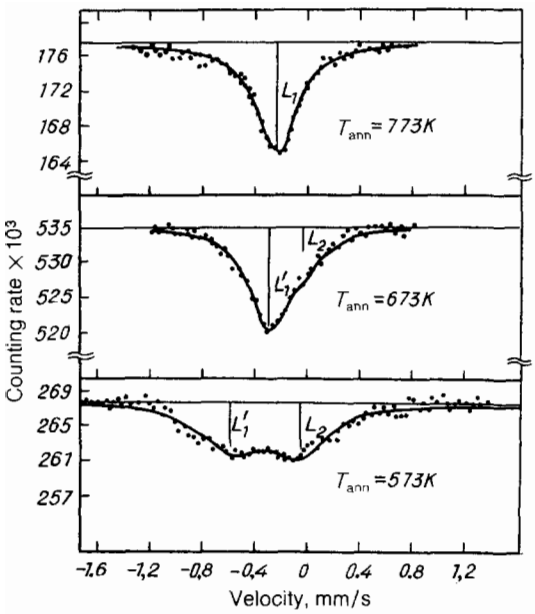

FIG. 13. Influence of the diffusion annealing temperature on the NGR spectra of ^{57}Co in grain boundaries in Pd.

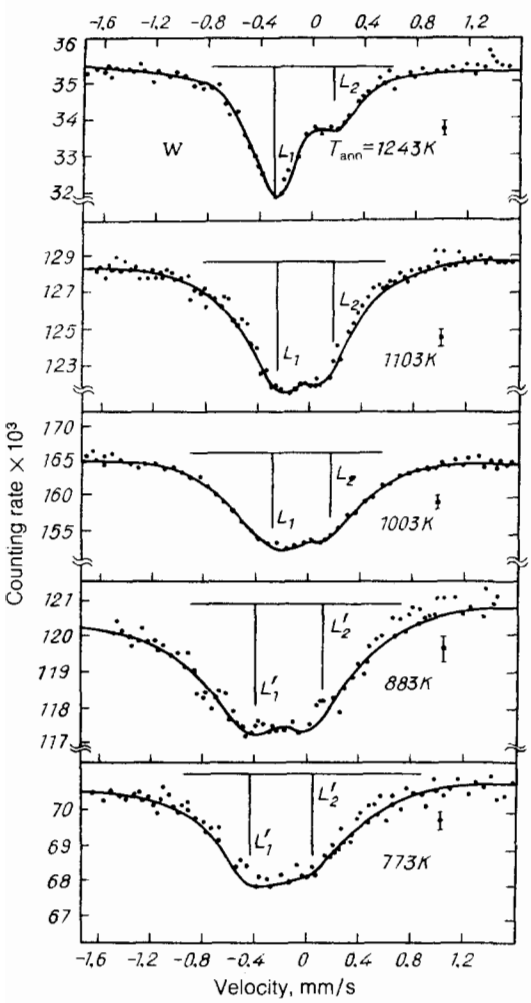

FIG. 14. Influence of the diffusion annealing temperature on the NGR spectra of ^{57}Co in grain boundaries in *W*.

obtained after diffusion annealing at different temperatures. Two important points should be stressed because they govern the quality of the experimental results. Firstly, some of the Pt and Pd matrices investigated by us can dissolve cobalt in any amounts. Therefore, in the case of these solvents there should be no problems due to the appearance of undesirable components of the NGR spectra because of the formation of cobalt atom clusters. Secondly, the results reported in this section were obtained by annealing at gradually increasing temperatures. The use of the same sample in plotting the dependences of the parameters of the NGR spectrum on the diffusion annealing temperature makes it possible to obtain the relationships under discussion.

It is clear from these spectra that the forecasts given above are at least partly justified. The area under the line, dominant at high temperatures, decreases as a result of cooling. We can therefore assume that this is the L_1 line. The area under the only new component, which can be attributed naturally to the states at grain boundaries and is called the L_2 line, increases as a result of cooling.

Before considering the quantitative dependences of the areas under the NGR lines on the diffusion annealing temperatures, we must point out an important circumstance. The forecasting of the clinical picture of the NGR spectra of polycrystalline samples is based on the hypothesis that this spectrum contains components associated with grain boundaries when the number of atomic probes in the boundary itself and in the adjoining zone of the regular lattice become comparable. Allowing for the linearity of the scale of intensities in NGR spectroscopy, we can assume that the expected *appearance of grain-boundary lines* in the NGR spectrum of a polycrystalline sample occurs when the number of the atomic probes in the boundaries P_{gb} becomes larger than, for example, $0.1P_{bk}$, where P_{bk} is the number of atomic probes in the bulk "pumping out" zone. In the first approximation, we shall assume that the bulk diffusion parameters of our atomic probes and the self-diffusion parameters are practically identical for platinum, which is justified to some extent by the unlimited solubility of cobalt in platinum.

We can easily see that the condition $P_{gb} = 0.1P_{bk}$ can be transformed in a natural manner to the condition

$$c_{gb}d = 0.1c_{bk}\cdot 2(D_{bk}t)^{1/2}, \tag{23}$$

where c_{gb} and c_{bk} are the average concentrations in the investigated regions, and d is the width (thickness) of a grain boundary. Bearing in mind the boundary conditions for PGBD given in Sec. 2.2, we shall assume that the average concentration in the bulk "pumping out" zone is approximately $0.5c_{gb}$. We then have

$$d \approx 0.1(D_{bk}t)^{1/2} \tag{24}$$

at the temperature of appearance of the grain-boundary component in the NGR spectrum of a polycrystalline sample.

Using the most reliable data on the self-diffusion parameters in platinum[55] ($D_0 = 0.0063$ cm^2/s and $Q = 6.2$ kcal/mol), we find that for $(1/T)^{-1} = (1.3\times 10^{-3})^{-1} = 769$ K and the annealing time of 7.2×10^3 s we obtain

$$d \approx 3\cdot 10^{-9}\ \text{cm} \leqslant 10^{-8}\ \text{cm}. \tag{25}$$

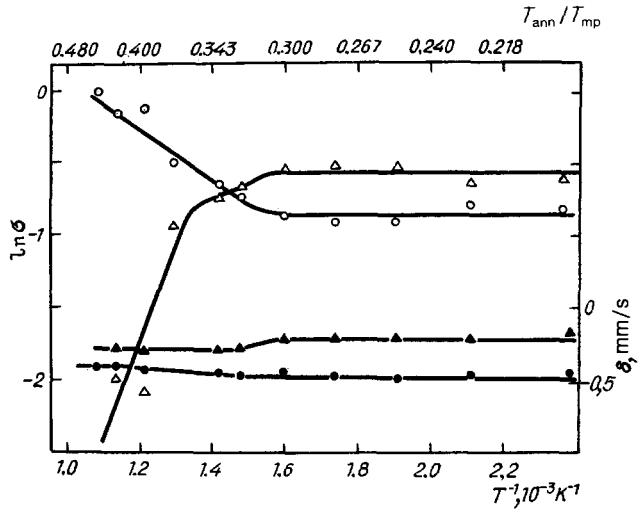

FIG. 15. Temperature dependences of ln $\sigma(\xi)$ and of $\delta(\xi)$ for ^{57}Co in grain boundaries in Pt.

Therefore, using the most general ideas on the mechanism of formation of the NGR spectra of polycrystalline samples, we can estimate the effective width of a grain boundary in a recrystallized polycrystalline sample, which is practically identical with the lattice parameter of platinum.

We shall now consider the quantitative relationships governing changes in the NGR spectrum due to changes in the diffusion annealing temperature. Figure 15 shows the dependences of the logarithms of the areas under the NGR lines on the reciprocals of the diffusion annealing temperatures in the case of Pt. We can see that lowering of the annealing temperature causes a practically linear reduction in the intensity of the L_1 line, whereas the intensity of the L_2 line rises linearly and rapidly up to a certain temperature below which the relative intensities of the lines remain constant. Before discussing this temperature dependence of the areas under the NGR lines, we shall first consider the dependences of the central shifts of the two components of the NGR spectrum of platinum on the reciprocal of temperature. We can see that in a wide range of temperatures the central shifts of the two components remain practically constant. This is evidence of constancy of the states observed in the range of temperatures accessible to NGR spectroscopy. The dependence obtained has an interesting feature in the form of a "triple point" temperature at which the normalized areas $\sigma(L_1)$ and $\sigma(L_2)$ of the two components become equal. Above the triple point temperature we are dealing with unchanged states in the grain boundary and in the adjoining region of the regular lattice the populations of these states vary with the diffusion temperature. In estimating the populations of these states we shall use the correct but fairly simple approximation[15,16] for the description of the distribution of the diffusant in the PGBD zone. In this approximation the diffusant concentration in the grain boundary itself is

$$c_{gb} = c_0 \exp(-\beta y) \tag{26}$$

and the concentration of the diffusant in the bulk "pumping out" zone is

$$c_{bk} = c_{gb} \operatorname{erfc}\left(\frac{x}{2(D_{pump}t)^{1/2}}\right); \tag{27}$$

here,

$$\beta = \left[\frac{2}{dD_{gb}}\left(\frac{D_{pump}}{\pi t}\right)^{1/2}\right]^{1/2}$$

The total amount of the diffusant in the PGBD zone (which is equal to the amount P_{bk} in the "pumping out" zone at temperatures $T > 0.45T_{mp}$) is described by

$$\sigma_1 = \int_{-\infty}^{\infty} dx \int_0^{\infty} c_{bk}\, dy = 4c_0(\pi^{-1}D_{pump}t)^{1/2}\beta^{-1}. \tag{28}$$

For this L_1 component $(0.45T_{mp} < T)$ when $(D_{pump}t)^{1/2} \gg d$ the enthalpy of activation is

$$Q(\sigma_1) = -\frac{d\ln\sigma_1}{d\xi} = \frac{Q_{gb}}{2} + \frac{Q_{pump}}{4}. \tag{29}$$

Hence, it follows that lowering of the diffusion saturation temperature causes σ_1 to decrease exponentially and the enthalpy of activation is high. However, the dependence (28) cannot be observed because of the absence of other components in the NGR spectrum of polycrystalline samples at these high temperatures.

We shall now consider the temperature range $0.35T_{mp} < T < 0.45T_{mp}$ where we can expect comparable populations of the grain-boundary "pumping out" states because of the relationship

$$d \approx (D_{bk}t)^{1/2};$$

here,

$$\sigma_1 = \int_0^{\infty} c_{gb}F(D_{pump}, d, x)\, dy = 4c_0\beta d\Phi. \tag{30}$$

In this temperature range the enthalpy of activation $Q(\sigma_1)$ is considerably smaller than that given by Eq. (29), as is indeed confirmed in Fig. 15.

It follows from Eq. (26) that

$$\sigma_2 = \int_0^{\infty} c_{gb}\, dy = c_0 d\beta^{-1}. \tag{31}$$

Hence, the enthalpy of activation is

$$Q(\sigma_2) = -\frac{d\ln\sigma_2}{d\xi} = \frac{Q_{pump}}{4} - \frac{Q_{gb}}{2}. \tag{32}$$

Therefore, if ln σ_2 rises on increase in ξ, then $Q(\sigma_2) < 0$ and $Q_{gb} < Q_{pump}/2$, as pointed out already in the discussion of the experimental results on PGBD in Sec. 2.

The physical meaning of the temperature at which in Fig. 15 there is a characteristic triple point follows from the above estimate given by Eq. (25): the bulk "pumping out" mechanism of atomic probes diffusing along grain boundaries is suppressed completely at the triple point.

We shall consider one more empirical test for an identification of the two components in the NGR spectra. This involves changes in the populations of the relevant states as a result of variation of the annealing temperature of a sample with an established population of two types of state. If the temperature of the subsequent annealing is less than the temperature at which a given population was established, there

TABLE V.

Host lattice	V	Nb	Ta	Cr	Mo	W	Rh	Ir	Pd	Pt
δ^{HT} (L_1)	+0.07	−0,03	−0.07	+0.12	−0.09	−0.18	−0.24	−0.32	−0.22	−0.40
δ_{publ}	+0.07	−0,02	−0.07	+0.12	−0,10	−0.20	−0.17	−0,30	−0,22	−0.40

should be no redistribution of the populations. Diffusion migration along a boundary should not alter the distribution between the states. Diffusion from the bulk "pumping out" zone back to the grain boundary at lower temperatures against the concentration gradient created by the initial annealing at a higher temperature cannot then take place.

Therefore, the states formed at higher temperatures are irreversible when annealing takes place at lower temperatures. On the other hand, the upward shift on the temperature scale should ensure a transition from states typical of low temperatures to those which form at higher temperatures. This is due to the fact that the direction of changes in the populations of these two types agrees with the direction of the concentration gradient near the boundary and with the direction of increase in the effective transport of the atomic probes increase in temperature.

We indeed observed irreversibility of the NGR spectra on transition from high-temperature states to those at lower temperatures. However, in the case of the transition in the opposite direction the spectra were very easily reproducible. This was used by us to suppress the scatter of the experimental dependences by using just one sample and subjecting it to heat treatments at gradually increasing temperatures, so that the initial distribution between the states was created by the diffusion annealing at the very lowest temperature.

Since our ideas on the relationships governing PGBD have made it possible to analyze qualitatively the observed changes of the relative intensities of two components in the NGR spectra only between the appearance of the grain-boundary component and the temperature of the kink (triple point temperature), defined above, all further discussion of the bulk of the experimental results will concentrate on these states.

3.2. Nature and properties of the L_1 states responsible for the main component of high-temperature grain-boundary NGR spectra

The relationships used by us were:

the dependence of the area under the L_1 line on the diffusion annealing temperature;

the ability to alter the states created earlier, depending on the direction of change in the annealing temperature, can reveal the L_1 component of the NGR spectra since it is due to the states of the atomic probes in regions of the regular lattice adjoining the grain boundary. If this is true, then all the other properties of this component, which can usually be determined by NGR spectroscopy, should be identical with the corresponding properties of the bulk NGR lines.

Table V gives the central shifts (δ) of the L_1 lines in all the host lattices which we investigated and lists either our own or published data on the central shifts of single paramagnetic lines observed for samples in which the diffusion process was carried out at temperatures typical of the preferential bulk diffusion in these host lattices. Clearly, these central shifts agreed excellently, providing one further argument in support of our classification.

We shall now consider the dynamic properties of the L_1 states. The information on the dynamic properties of atomic probes was obtained by determination of the temperature dependences of the NGR probability (by finding the areas of the relevant component normalized to the whole area under the NGR spectrum) in the temperature range 5–300 K. Figure 16 shows, by way of example, the relevant dependence in the case of palladium. We can see that this metal exhibits an unexpected anomaly: cooling does not increase the NGR probability, but reduces it and in the case of palladium the temperature of the onset of the fall is close to the room value. The nature of this anomaly was studied by recording the spectra of our samples at helium temperatures, but on a velocity scale which was highly compressed.

Figure 17 shows the recorded spectra. We can see that at low temperatures the states of the atomic probes discussed by us become ferromagnetically ordered. In host lattices such as palladium, this results in a fairly strong field on the nuclei, so that a characteristic sextet of lines is observed, and rhodium and iridium exhibit only line broadening indicating that the fields are much weaker at the cores. Naturally, on a compressed velocity scale we determined the most typical NGR spectra and established that the observed "anomalous" reduction in the line intensities as a result of a reduction in the measurement temperature is a simple consequence of its "transfer" from the only paramagnetic line to the components of the sextet. Consequently, we can now do the following:

measure the total area under the spectrum on a compressed velocity scale, determine the required temperature dependence of the L_1 line, and calculate the corresponding dynamic characteristics of the L_1 states;

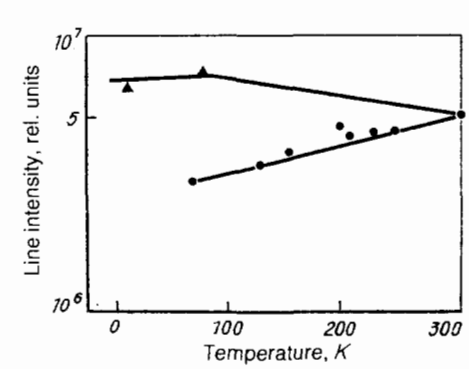

FIG. 16. Dependence of $\sigma(L_1)$ on the temperature of measurement of NGR spectra of ^{57}Co in grain boundaries in Pd.

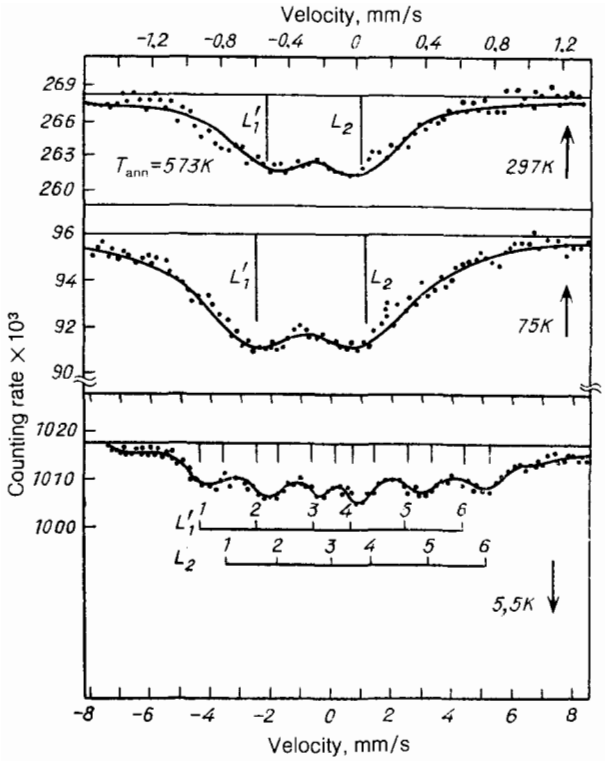

FIG. 17. Influence of the measurement temperature on the NGR spectra of ^{57}Co in grain boundaries in Pd.

use the magnetic ordering characteristics to obtain new and unique information on the areas of the regular lattice adjoining grain boundaries and extending to distances not exceeding $2(D_{\text{pump}}t)^{1/2} \approx 10^{-8} - 10^{-7}$ cm. We shall complete the identification of our L_1 states by considering the results presented in Table VI. In addition to the characteristic Debye temperatures $\Theta(L_1)$ of the L_1 states, this table gives also the published values of the Debye temperatures for the corresponding bulk spectra. We can see from the published Debye temperatures deduced from the NGR probability (Θ_f) and from the magnitude of the second-order Doppler shift (Θ_δ) that they are very different, although we always have $\Theta_f > \Theta_\delta$. With the exception of rhodium, this is true of the L_1 line for many metals. However, on the whole the agreement between our measured dynamic characteristics of the L_1 states with the published data is quite acceptable and it provides a further argument in support of the hypothesis that the L_1 line is due to the states in the regular lattice in the vicinity of grain boundaries.

We shall now consider the characteristics of ferromagnetic-ordering associated with the L_1 states. As is known, it is these matrices that can exhibit paramagnetic ordering of dilute solid solutions of magnetically active impurities.[67] The magnetic order in such systems is due to the indirect exchange mechanism in which conduction electrons of the host lattice participate actively. The Curie point of such very dilute solid solutions is described by[67]

$$T_c = (12\mu_B)^{-1} c_i (s+1) s\chi_0 a^2, \tag{33}$$

where μ_B is the Bohr magneton; c_1 is the bulk concentration of the impurities; s is the spin quantum number; χ_0 is the paramagnetic susceptibility of conduction electrons in the matrix; a is a constant.

The paramagnetic susceptibility of conduction electrons in the matrix is directly proportional to the concentration of these electrons, which suggests a way of obtaining additional microscopic information on the investigated states. Before considering the estimates, we shall identify the impurities responsible for the ferromagnetic ordering involving the L_1 states: we have to determine whether these are the residual magnetically active impurities or those impurities which reach such regions together with the atomic probes as a result of PGBD. The compositions of our samples were determined by the method of secondary-ion mass spectroscopy using IMS–3F and Cameca (made in France) spectrometers after completion of all the other measurements, so as to identify the impurity contamination which might happen during diffusion annealing. The total concentration of the 3d impurities in Pt should not exceed 130 ppm, whereas in Pd it should not exceed 100 ppm.

If we use the familiar dependences of the Curie temperatures of such solid solutions on the concentration of magnetically active impurities, we can estimate[56] the concentrations of residual impurities in the zone of localization of the L_1 states. It is clear from Table VII that in order to determine the temperatures $T_c(L_1)$ it is sufficient to enrich the corresponding regions with the relevant impurity to 4–10 at.%, which is much higher than the average composition in these materials. It should be mentioned that in the case of these systems it has been predicted theoretically and confirmed experimentally[57] that the impurities representing the 3d transition metals (iron, cobalt, and nickel) do not become segregated in rhodium, palladium, iridium, and platinum host lattices. Consequently, we can ignore residual magnetically active impurities.

One further possibility of a strong increase in the concentration of magnetically active impurities near grain boundaries is the fact that these impurities are supplied together with the atomic probes. Then, the average concentration determined by the secondary-ion mass spectroscopy technique is effectively localized in a zone 2 of $(D_{\text{pump}}t)^{1/2}$, so that for the grain size of 2×10^{-3} cm the concentration increases by a factor of 10^3–10^4. This is quite sufficient to ensure 10 at.% in the "pumping out" zone when the average measured concentration is 100 ppm.

TABLE VI.

Host lattice	Pd	Pt	Rh	Ir
$\Theta_f^{HT}(L_1)$	400	420	380	440
$\Theta_\delta^{HT}(L_1)$	330	320	430	400
Θ_f (publ.)	370	360	430	460
Θ_δ (publ.)	250	270	400	400

TABLE VII.

Host lattice	Pd	Pt	Rh	Ir
$T_c^{HT}(L_1)$	280	240	100	100
$H^{HT}(L_1)$	31.5	31.5	19.0	7.5
c (Fe), at.%	12	10	—	—

TABLE VIII.

Host lattice	V	Nb	Ta	Cr	Mo	W	Rh	Ir	Pd	Pt
δ^{HT} (L_2)	0.26	0.69	0.30	−0.09	0.58	0.30	0.03	−0.05	—	−0.20
δ_{21}^{HT}	0.19	0.72	0.42	−0.21	0.68	0.48	0.20	0.22	—	0.21

Unfortunately, we cannot use just NGR spectra to find the high concentration of 3d transition impurities in the grain boundary itself and in the adjoining regions of the regular lattice. In fact, as shown in Refs. 58 and 59 the isomeric shifts of the NGR lines are not very sensitive to the solid-solution composition. For example, in the case of solid solutions based on copper the maximum effect is 1.8×10^{-2} mm s^{-1}(at.%)$^{-1}$, whereas in the case of solid solutions of Fe in platinum there are no changes in the isomeric shift in the range of concentrations of interest to us if the impurity atom is not the nearest neighbor of an atomic probe.

3.3. Nature and properties of the L_2 states representing the second component of high-temperature grain-boundary NGR spectra

It was shown in Sec. 2 that the current ideas on the process of PGBD, used by us to supply atomic probes to the cores of structure defects of the grain-boundary type, makes it possible to identify the L_2 component in high-temperature NGR spectra as due to the states of the atomic probes in grain boundaries along accelerated diffusion paths. If we adopt this hypothesis, we can discuss the available information on the states in grain boundaries discovered by us.

First of all, we must mention once again that in all the investigated host lattices containing recrystallized boundaries we observed NGR spectra of ^{57}Fe consisting of just two components: one L_1 component discussed already, and the other L_2 component which in all cases corresponded to the atomic probe states in the grain boundaries, in accordance with empirical criteria used by us. The observed "lack of opportunity" of placing our atomic probe within the grain boundaries may be due to two circumstances:

the fundamental limitation on the number of sites or positions in the core of a grain boundary capable of accepting an impurity of a given type;

selection of the diffusion path with a minimum enthalpy of activation, which is used as the atomic probe in the course of its delivery with the aid of PGBD.

The relationship governing the change in σ (Fig. 15) representing an exponential increase as a result of cooling, is an important qualitative argument in support of the hypothesis that the L_2 states are due to localization of the atomic probes along the accelerated diffusion paths in grain boundaries.

We shall now consider one of the principal parameters of an NGR line, which is the central shift of the L_2 lines. Table VIII gives the values of $\delta(L_2)$ for all the investigated host lattices. It is clear that, with the exception of chromium, the difference between the central shifts $\delta(L_2)-\delta(L_1)=\delta_{21}$ in these lattices is positive. Using the current ideas on the nature of the isomeric shift of NGR lines,[60,61] we may conclude that such identical behavior of δ_{21} in so very different lattices can be due to one feature common to both systems: the atomic probe reaches the states at grain boundaries, the volume of which is considerably smaller than the volume of the atomic probe. Compression of the ^{57}Fe ion at these positions then increases the density of the intrinsic s electrons near the NGR nucleus, as demonstrated by the positive value of δ_{21}.

Only in the case of chromium, for which the atomic volume of the host lattice is equal to the atomic probe volume, is the isomeric shift negative.

It therefore follows that in the core of a grain boundary in the majority of the metals investigated by us the ^{57}Fe atomic probes occupy either interstitial positions or sites in the regular structure at which the volume is reduced not only for the host lattice atoms, but also for the atomic probes which are considerably smaller. According to the dislocation model of the grain-boundary structure, such states correspond either to positions under the edge of an extra half-plane in an edge dislocation (interstitial positions) or to sites in the last row of the extra half-plane where the compressed region of the core of an edge dislocation is located. The first type of states under the edge of the extra half-plane is in good agreement with the hypothesis of possible accelerated diffusion paths along dislocations and grain boundaries.[62] The second type of states at the edge of the extra half-plane is in conflict with the simplest ideas on the vacancy mechanism of diffusion in such one-dimensional structures. Alternately, the second type of states can be regarded as representing traps for atomic probes diffusing rapidly between positions of the first type. However, this is in turn in conflict with the uniqueness of the L_2 line and the uniqueness of the associated state, because it is difficult to see how the instantaneous concentration of the atomic probes in fast diffusion channels could be much less than their concentration in the traps under any conditions during diffusion annealing.

We shall now consider other characteristics of the L_2 states. As in the case of the L_1 states studied earlier, we investigated the influence of temperature on the NGR spectra in the range 5–300 K. Figure 18 shows the dependences

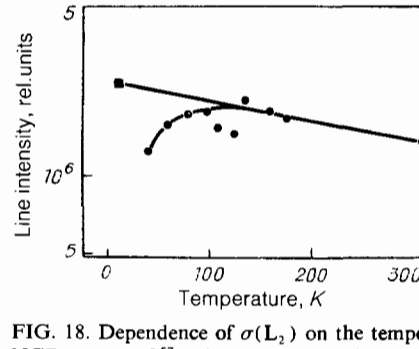

FIG. 18. Dependence of $\sigma(L_2)$ on the temperature of measurement of NGR spectra of ^{57}Co in grain boundaries in Pd.

TABLE IX.

Host lattice	Pd	Pt	Rh	Ir
Θ_f^{HT} (L_2)	250	220	240	210
Θ_{21}^{HT}	—150	—200	—140	—230

$\sigma_2(T)$. Exactly as in the case of the L_1 states, there are anomalies which disappear if we allow for the ferromagnetic ordering at low temperatures. Table IX lists the dynamic characteristics of the L_2 states. It follows from the differences between the characteristic temperatures of the L_2 and L_1 states that in all cases without exception the dynamic characteristics of the atomic probes in grain boundaries have considerably smaller values than in the bulk. Bearing in mind the conclusions reached earlier about the nature of the positive isomeric shift of the L_2 states, we have to admit that some of the possibilities discussed above must be rejected because they do not agree with the new observations. In fact, if the atomic probes in the grain boundaries are compressed (positive isomeric shift), then the frequencies of their local vibrations should increase because of a reduction in the interatomic distances which occurs at the time of compression of the environment. The observed combination of the properties—the interstitial-like positions and the spectrum of local vibrations of the atomic probes with lower frequencies—are typical of a familiar point defect, which is a split host lattice or mixed interstitial.[63] Experiments and theoretical analysis of the properties of these point defects have shown that the spectrum of local vibrations of such a complex defect has a resonance band at the bottom of the phonon spectral band, which is responsible for the familiar anomalies of crystals with such defects and for the high mobility of these defects at near-helium temperatures.

It is stressed repeatedly above that the atomic probe used by us has an unlimited solubility in the group VIII elements. This undoubtedly confirms that the probe impurity forms substitutional solid solutions in the investigated elements. In the case of grain boundaries the need to reconcile the positive isomeric shift of the L_2 states with the low dynamic characteristics of these states makes it necessary to introduce the hypothesis that in the core of a grain boundary our atomic probe occupies split mixed interstitial positions. Unfortunately, in the systems we studied the properties of radiation defects had not been investigated by the NGR method, in contrast to the major cycle of studies carried out by Prof. G. Vogl and his colleagues.[64-66] A direct comparison of the properties of mixed dumbbells formed in electron-irradiated Pt (investigated using the ^{57}Co probe) with our grain-boundary NGR spectra should make the situation clear.

TABLE X.

Host lattice	Pd	Pt	Rh	Ir
T_c^{HT} (L_2)	—	80	100	80
T_{21}^{HT}	—	—160	0	—20
H^{HT} (L_2)	—	315	190	70
H_{21}^{HT}	—	0	0	0

We shall now consider magnetic properties of the L_2 states. Table X lists the magnetic characteristics of the L_2 states described as above: this table gives the Curie temperatures deduced from the onset of the anomalous behavior of the NGR probability as a result of lowering of the temperature at which the NGR spectra were measured (see Fig. 18) and the effective field at the nuclei deduced from the separation between the components of a sextet measured at 5.5 K. Table X includes the values of the ferromagnetic impurity concentration (for example, iron) calculated formally from the dependences of the bulk Curie temperature on the concentration of magnetically active impurities in solid solutions based on platinum or palladium. Table X gives also the differences between the Curie temperatures and the effective magnetic fields at the nuclei for the purpose of comparison of the properties of the L_2 and L_1 states. Clearly, in all the investigated metals both the Curie temperatures and the effective fields at the nuclei are lower for the L_2 states than for the L_1 states. What is the reason for this difference? As already discussed in the preceding section, there is only one way that the concentration of an accidental magnetically active impurity can increase in a grain boundary and in the regular lattice next to it: this is diffusion of these impurities together with the atomic probes. In this case the impurity responsible for the observed ferromagnetic ordering is distributed in such a way that this maximum concentration is localized exactly at the grain boundary for reasons which should be obvious. It then follows unambiguously that the characteristics of the electron spectrum of the grain boundaries themselves or, more exactly, of the regions occupied by the localized states responsible for the appearance of the L_2 components in the NGR spectra differ considerably from the characteristics of the parts of the lattice adjoining a grain boundary. If it is permissible to use Eq. (33) to describe the magnetic ordering along the accelerated diffusion paths of the atomic probes, we can conclude that the *paramagnetic susceptibility of conduction electrons in grain boundaries* is considerably *less* than in the adjoining parts of the lattice. In the strongly degenerate limit the paramagnetic susceptibility of electrons in a metal is given by[67]

$$\chi_{el}^{par} \sim m\mu_B^2 n^{1/3}, \tag{34}$$

where μ_B is the Bohr magneton; n is the conduction electron density; m is the electron mass.

The values of T_{21} and H_{21} given in Table X imply that the conduction electron density averaged in the plane of a grain boundary at distances of the order of the separation between the magnetically active impurities is less than the conduction electron density in the regular lattice.

All this evidence makes it possible to draw the following important conclusions:

the ferromagnetic ordering of the L_2 states in grain boundaries occurs at lower temperatures and cannot be due to a lower concentration of the magnetically active impurities in the core of a grain boundary;

this lowering of the ferromagnetic transition temperature in L_2 states is due to a reduction in the average value of the conduction electron density because the conduction electrons are responsible for the ordering in the bulk of such solid solutions;

we cannot exclude the possibility that the change in the

symmetry and the interatomic distances within the core of a grain boundary (in cores of grain-boundary dislocations) is the reason for the appearance of the band magnetism in these cores.

We shall conclude this subsection by drawing attention to the apparent conflict between the properties of the L_2 states. In fact, if—as can be deduced from the magnetic characteristics of the L_2 states—the average value of the conduction electron density in the region where the L_2 states are localized is less than in the adjoining regions of the regular lattice, then why does the majority of the investigated host lattices exhibit a positive central shift indicating a local increase in the density of the s electrons near the nuclei of the atomic probes? This apparent conflict can be resolved by assuming that the higher density of the s electrons at the nuclei and the positive isomeric shift are due to the compression of the inner shells of the atomic probe ions. The lower average conduction electron density in this region has practically no influence on the isomeric shift. It therefore follows that:

an atomic probe in the form of ^{57}Co inside the core of a grain boundary (in a core of a grain-boundary dislocation) is in a special L_2 state which has properties very different from the ^{57}Co states at the sites of the regular lattice (L_1 states);

the L_2 states represent the accelerated diffusion paths along grain boundaries (within cores of grain-boundary dislocations);

the L_2 states are of the interstitial type because the positive isomeric shift of the L_2 lines in the NGR spectra is due to the corresponding compression of the electron shells of the atomic probe ion;

the spectrum of the local vibrations of the atomic probe in the L_2 state is considerably softer than at the regular lattice sites (in combination with the conclusion on the interstitial position of the atomic probe in the L_2 state, this means that the atomic probes in grain boundaries are not single-particle interstitials but form a mixed split configuration which is known to be characterized by a wide resonance mode at the bottom of the vibrational spectral band);

at sufficiently low temperatures in the region where the L_2 states are localized we can expect a ferromagnetic transition resulting in the splitting of the NGR spectrum into characteristic sextet lines (the parameters of this transition demonstrate a *reduction in the average electron density in the region of localization of the L_2 states*);

all these results demonstrate that our method for obtaining microscopic information on the structure and on the electronic and dynamic properties of grain boundaries and dislocations *opens up completely new opportunities for the investigation of local properties* of these important components of the structure of a real crystal.

3.4. Origin and properties of the states of atomic probes investigated under conditions of low-temperature diffusion in polycrystalline metals

In the preceding subsections we discussed the properties and the origin of the impurity states occupied by our atomic probes after high-temperature diffusion annealing in the range $0.35T_{mp} < T$. As pointed out already, we discussed the states responsible for the NGR lines with areas under them varying rapidly with the diffusion annealing temperature. However, it was found that when a certain temperature (triple point) is reached the changes in the areas under these NGR lines cease (Fig. 15) and at all lower temperatures the equality of the two components of the NGR spectra of polycrystalline samples reached at the triple point is retained. This gives rise to the following question: are the low-temperature states new and different from the high-temperature states? If we turn back to Fig. 15, we can see that in the first approximation the isomeric shifts of the two components of the NGR spectra of polycrystalline samples remain practically constant. This is a very important argument in support of the hypothesis that there is no change in the nature of the states responsible for the two components of the NGR spectra of polycrystalline samples and it provides the basis of seeking the reason why the changes in the areas under the L_1 and L_2 lines cease at low temperatures.

The very constancy of the areas under the NGR lines in a wide range of diffusion annealing temperatures simply means that the following inequality applies in this range:

$$Q_{gb} = Q_{pump}. \tag{35}$$

which was discussed already in Sec. 2 in connection with the kinks of the temperature dependences of the grain-boundary self- and heterodiffusion coefficients representing migration in silver and nickel. In that section we considered the rapid transition from the bulk "pumping out" mechanism, which is characterized by

$$Q_{pump} = Q_{bk} \tag{36}$$

to a new mechanism of this phenomenon when the relationship of Eq. (35) is satisfied and we put forward the hypothesis that at sufficiently low temperatures we can expect activation of the dislocation "pumping out" mechanism for which the relationship of Eq. (35) is a natural consequence. This dislocation "pumping out" hypothesis based simply on the data on the parameters of PGBD is fully justified, because these parameters are always affected by the characteristics of diffusion along actual grain boundaries and by the characteristics of the "pumping out" of the diffusant from the boundaries, so that they cannot be separated. We now have completely independent information on the states within a grain boundary and on the states in the "pumping out" zone, so that we can identify the cause of the relationship (35) at low temperatures instead of the usual generally accepted relationship (36), which undoubtedly applies at relatively high temperatures. It should be stressed that the hypothesis of the dislocation "pumping out" and the assumptions under this treatment are based on the observation that the diffusion flux in PGBD remains two-dimensional at all the temperatures investigated so far. This means that there is always one or another mechanism which can give rise to "pumping out" of the diffusant from grain boundaries and this is naturally the reason for the characteristic always—observed linear dependence $\ln C(y)$ (see Figs. 1 and 2), instead of $\ln C(y^2)$ which applies to diffusion in a homogeneous medium.

We have discussed several times the importance of the triple point temperature on the dependence in Fig. 15 from the point of view of diffusion: at this temperature the effective diffusion length $(D_{pump}t)^{1/2}$ of an atomic probe in the

"pumping out" zone becomes of the order of the lattice parameter, which is 10^{-8} cm. It is at this temperature that there is a change in the "pumping out" mechanism and Eq. (36) begins to apply. Consequently, it is the properties of a monatomic layer adjoining a grain boundary that are responsible for the observed changes in our clinical picture of PGBD and for the change to the horizontal dependence in Fig. 15. Thus, if the contribution of the first atomic layer adjoining a grain boundary becomes dominant in diffusion migration of an atomic probe outside the boundary, there is a rapid change in the observed parameters of the "pumping out" process. It is natural to assume that it is the *change in the properties of this layer* adjoining a grain boundary that are responsible for the appearance of the relationship (35). What are the properties of a regular lattice adjoining a grain boundary which change in such a drastic manner as to halve the enthalpy of activation of the diffusion of atomic probes migrating out of the boundary into this layer? We must postulate the following:

such a strong reduction in the potential barrier in this layer that, for a constant vacancy concentration, the enthalpy of activation is approximately halved;

an increase in the vacancy concentration in the part of the lattice adjoining a grain boundary to such an extent that the diffusion in this region is governed no longer by the equilibrium vacancy concentration in the lattice, but by the local concentration of vacancies in this region.

It seems to us that there are no factors which could alter so greatly the potential relief of the lattice near a grain boundary. If the elastic distortions present in this region can change to any significant degree the height of the potential barriers to diffusion, then the changes can only be of the order of the second-order corrections. As far as the increase in the concentration of vacancies in this region is concerned, it seems at first sight that we have a familiar and physically justified mechanism: internal adsorption of vacancies (vacancy segregation) at the structural inhomogeneities, including those at grain boundaries. However, the enthalpies of activation of segregation of vacancies at grain boundaries or at dislocations known at present[19] amount to about 0.2–0.5 eV (5–12 kcal/mole) which cannot naturally account for the relationship $Q_{\text{pump}} \approx Q_{\text{gb}}$ observed experimentally in this range of temperatures. In fact, if we assume that all the changes in the diffusion properties in a thin layer of adsorption accumulation of vacancies near a grain boundary are entirely due to an increase in the vacancy concentration as a result of segregation, then the enthalpy of activation of self-diffusion in this layer simply decreases by an amount equal to the enthalpy of segregation, which is quite insufficient to explain the results.

We must find such a mechanism of a change in the diffusion properties which would at least reduce to zero the enthalpy of formation of vacancies in this monatomic layer adjoining a grain boundary. Since in the case of fcc metals we have $H^{\text{f}} > H^{\text{m}}$ the mechanism responsible for $H^{\text{f}} \approx 0$ should not be in conflict with the observations.

Fortunately, such a mechanism is known. It is the formation of strongly bound impurity–vacancy complexes which ensure that at sufficiently high values of the enthalpies of activation of binding the low-temperature concentration of vacancies becomes so high that self-diffusion in such crystals containing impurities is characterized by an activation enthalpy that does not contain the enthalpy of vacancy formation. These properties of self-diffusion in the "impurity region" have been investigated thoroughly for diatomic ionic crystals in which the energies of binding of vacancies to polyatomic impurities are quite high. It has been assumed that such a situation cannot occur in metals. However, as shown in Refs. 68 and 69, in the case of platinum and nickel in which the solubility of carbon can reach 10 at.% for platinum and 2 at.% for nickel the carbon–vacancy binding energies are 0.6–0.8 eV. In the case of platinum it is found that vacancy–carbon complexes are localized near grain boundaries,[69] where—as pointed out by the author—the diffusion due to vacancies is accelerated strongly in the presence of these complexes. We cannot exclude the possibility that even higher energies of binding to vacancies apply to oxygen—vacancy or nitrogen—vacancy complexes that have not yet been investigated. Bearing in mind that the elastic interactions of these impurities can only increase the binding energies with vacancies, we shall assume that our samples contain vacancy–interstitial impurity complexes with binding energies 1.0–1.2 eV (23–28 kcal/mol). Consequently, a layer of adsorption accumulation of impurities and vacancies adjoining a grain boundary may contain strongly bound complexes which are responsible for the appearance of a range of temperatures where "impurity diffusion" is observed and its properties are similar to those of similar diffusion in ionic crystals when the enthalpy of activation of the vacancy diffusion mechanism decreases approximately twofold to the value of the enthalpy of activation of vacancy migration.

3.4.1. Properties of low-temperature L_1 states. If the above explanation of the nature of the low-temperature L states is correct, then sufficiently heavy doping of the layer adjoining a grain boundary should be manifested also by changes in other parameters of NGR spectra. We all consider first the main property of NGR lines which is the central shift. Although we had assumed that the shift $\delta(L_1)$ is practically constant, a more careful analysis shows that $\delta(L_1)$ decreases with temperature in the region of the triple point. In view of the low sensitivity of δ to doping of solid solutions, mentioned already above, we may conclude that in this temperature range the adsorption accumulation layer is quite heavily doped, in full agreement with the above explanation. Moreover, our hypothesis that the adsorption accumulation layer concentrates an interstitial impurity generating impurity–vacancy complexes is in excellent agreement with the sign of the change in $\delta(L_1)$ below the triple point. Obviously, the interstitial impurity increases the lattice parameter. The atomic probes which reach this region migrate under conditions of effective stretching, compared with the lattice sites far from the grain boundary and from the adsorption accumulation layer. Therefore, the central shift of the L_1 states in such regions enriched with interstitial impurities should be more negative than at the regular lattice sites. Table XI gives the values of the central shifts of the L_1 states observed at temperatures below the triple point and the difference $\Delta\delta(L_1)$ of these shifts from the corresponding values for the L_1 states at temperatures above the triple point. We can see that the behavior described above for platinum is exhibited by all the metals investigated by us. Bearing in mind also the common properties of the systems formed by these metals, it seems to us that this behavior is natural.

TABLE XI.

Host lattice	W	Rh	Ir	Pd	Pt
δ^{LT} (L_1)	−0.40	−0.50	−0.55	−0.55	−0.50
$\Delta\delta$ (L_1)	−0.22	−0.23	−0.23	−0.33	−0.10

We shall now turn to the dynamic and magnetic properties of the low-temperature L_1 states. As before, the temperature dependences of the NGR probability exhibit "anomalous" reduction in this probability as a result of cooling, which is due to the appearance of ferromagnetic ordering within the grain boundary itself and close to it. An allowance for this redistribution of the intensities of the NGR lines suppresses the anomaly and makes it possible to determine the dynamic characteristics of these states. Table XII gives the characteristic Debye temperatures $\Theta_f^{LT}(L_1)$ of the low-temperature (LT) L_1 states and the differences between these Debye temperatures and the corresponding temperatures of the high-temperature states.

It is clear that in the case of all the host lattices the dynamic properties of the low-temperature L_1 states have lower values than those of the high-temperature L_1 states. This difference can be readily understood on the basis of the same hypothesis of heavy doping of the adsorption accumulation layer by interstitial impurities, since it is known that in solid solutions (such as those of carbon in metals) the interatomic interactions are weaker, as demonstrated by changes in the thermodynamic parameters of such solid solutions.

We shall now consider the magnetic properties of the low-temperature L_1 states. Table XIII gives the values of the Curie temperature of the low-temperature L_1 states, the differences $\Delta T_c(L_1)$, the effective fields at the nuclei of the atomic probes in these states, and the differences between them. It should be pointed out that for the reasons already discussed the magnetic parameters of rhodium and iridium have been determined subject to a relatively large error and this applies particularly to the Curie temperature T_c. It is clear from this table that the characteristics of the ferromagnetic state in the adsorption accumulation layer have considerably smaller values at low temperatures. This may be a consequence of heavy doping of the region in question with carbon or similar interstitial impurities. As is well known, solid solutions of Pt and Pd containing ferromagnetic impurities exhibit a reduction in the Curie temperature in the presence of any dopant.[70] However, it is possible that in such situations we are dealing with doping by a magnetically active impurity concentrated in grain boundaries and in the adjoining region by diffusion of such an impurity together with atomic probes.

We shall summarize once again our observations on the

TABLE XII.

Host lattice	Pd	Pt	Rh	Ir
Θ^{LT} (L_1)	320	400	310	370
$\Delta\Theta$ (L_1)	−80	−20	−70	−70

TABLE XIII.

Host lattice	Pd	Pt	Rh	Ir
T^{LT} (L_1)	130	100	110	100
ΔT (L_1)	−150	−140	+10	0

magnetic properties of the investigated impurity states in polycrystalline metals:

$$T_c^{HT}(L_1) > T_c^{HT}(L_2) \approx T_c^{LT}(L_2) \approx T_c^{LT}(L_1); \tag{37}$$

where the superscripts HT and LT identify high and low temperatures. It is known that

$$T_c \approx c_i\chi_0. \tag{38}$$

In subsequent estimates we shall write down the ratios of the populations (ratios of the concentrations of the atomic probes) characterizing the investigated states. It follows from Eqs. (28) and (31) that

$$c(L_1) = \frac{\sigma_1}{2(D_{\text{pump}}t)^{1/2}} = \frac{4c_0}{\sqrt{\pi}\beta} \tag{39}$$

$$c(L_2) = \frac{\sigma_2}{d} = c_0\beta^{-1}, \tag{40}$$

$$c(L_1) < c(L_2) \quad \text{at} \quad T = \text{const}. \tag{41}$$

We can now readily deduce the following obvious consequences. In the case of the L_1 state we have $T_c^{HT}(\lambda_1)/T_c^{LT}(L_1) = T_1^{HT}/T_1^{LT} \sim c_1^{HT}/c_1^{LT}$ because of the obvious equality $\chi^{HT} = \chi^{LT}$. Using Eq. (39), we obtain

$$\frac{T_1^{HT}}{T_1^{LT}} \sim \frac{c_1^{HT}}{c_1^{LT}} \sim \frac{\beta^{LT}}{\beta^{HT}}. \tag{42}$$

However, it is well known (see Sec. 2) that in the case of PGBD the quantity β increases rapidly as a result of cooling. Consequently, we find that

$$T_1^{LT} \ll T_1^{HT}, \tag{43}$$

in full agreement with Eq. (37). We shall consider the relationships applying to different states at the same diffusion annealing temperature:

$$\frac{T_1}{T_2} = \frac{\chi_1 c_1}{\chi_2 c_2}. \tag{44}$$

Since for $T = \text{const}$ we have $c_1 \leqslant c_2$, it follows that

$$\frac{T_1}{T_2}\frac{c_2}{c_1} = \frac{\chi_1}{\chi_2}. \tag{45}$$

At high temperatures when $(T_1/T_2)^{HT} > 1$, it follows that $\chi_1 \gg \chi_2$ and

$$n(L_1) \gg n(L_2). \tag{46}$$

The result for low temperatures when $(T_1/T_2)^{LT} \geqslant 1$ is in full agreement with the above estimates.

The main conclusion of our analysis is as follows: *the conduction electron density inside a grain boundary is lower than in the adjoining region of the regular lattice.*

We can therefore conclude that the low-temperature L_1 states differ from their high-temperature analogs only by the fact that they are localized in the zone of adsorption accumulation of vacancy–interstitial impurity complexes which is

diffusion-doped by a magnetically active impurity.

3.4.2. Properties of low-temperature L_2 states. We shall now consider the differences between the low-temperature L_2 states which distinguishes them from their high-temperature analogs. We shall proceed in the same way as in the case of the low-temperature L_1 states. There is no need to discuss the major changes in the diffusion properties in the region of localization of the L_2 states which are located in grain boundaries. Essentially, the constancy of the diffusion properties of the boundary is the basic hypothesis of our analysis. However, we must consistently allow for the consequences of the assumptions made above.

We shall consider the central shifts of the low-temperature L_2 states (Fig. 15). The central shift increases in the region of the triple point when the temperature is lowered and the value of δ then remains constant at a new higher level. If, as in the case of the low-temperature L_1 states, this change in the central shift at low diffusion annealing temperatures is due to doping, we have to conclude that low-temperature diffusion annealing makes grain boundaries doped preferentially with an impurity that reduces the interatomic states, increases the density of the s electrons in the nuclei of the atomic probes, and increases the central shift of the low-temperature L_2 line. This impurity is obviously iron which reaches the grain boundaries by diffusion together with the atomic probes.

Essentially both within the boundary and in the adjoining parts of the lattice we are faced with a competition between the changes caused by the interstitial impurity, which increases the lattice parameter, and the substitutional impurity, which reduces this parameter. In the lattice the interstitial impurity predominates, so that the changes in the interatomic distances caused by this impurity are considerably greater than changes induced by the substitutional impurity. Within the boundary this situation is more complex because of the presence of regions with different stacking densities.

Consequently, the interstitial impurities are located in "stretched" regions of the boundary and their influence on the interatomic distances and on the state of the atomic probes is greatly weakened. The substitutional impurity occupies a smaller atomic volume and is localized in "compressed" parts of the lattice exactly where the atomic probes are located, which is responsible for the predominant influence of this impurity on the isomeric shifts of the low-temperature L_2 states.

There is no doubt that the characteristics of the low-temperature L_1 states should differ from the characteristics of the high-temperature L_1 states because of two circumstances:

formation of vacancy–interstitial impurity complexes at relatively low temperatures governed by the binding energy of a complex;

reduction in the effective depth of the diffusion "pumping out" of the atomic probes until it becomes equal to the thickness of the adsorption accumulation layer, which naturally happens also at low temperatures.

A similar situation applies also to the low-temperature L_2 states. At low temperatures the "pumping out" zone is small and it is localized within the layer of adsorption of vacancy–interstitial impurity complexes. Therefore, although the number of the atomic probes in a sample is approximately constant, their concentration in a grain boundary is considerably higher at low temperatures and begins to fall above the triple point when the capacity of the "pumping out" zone increases greatly because the effective diffusion length now projects outside the thickness of the adsorption layer.

TABLE XIV.

Host lattice	Pd	Pt	Ir
Θ^{LT} (L_2)	250	240	210
$\Delta\Theta$ (L_2)	—	—20	0
Θ_{21}^{LT}	—70	—160	—160

We shall now analyze other properties of the low-temperature L_2 states. It is clear from Table XIV that the dynamic properties of the low-temperature L_2 states do not differ from the properties of the high-temperature L_2 states, although we would expect heavy doping of grain boundaries both as a result of the adsorption accumulation mechanism and also because of the diffusion doping. However, the transition to multiparameter conditions makes any detailed discussion pointless. It should be mentioned that the difference between the dynamic properties of the L_1 and L_2 states becomes smaller in this range of temperatures (Table IX) because of changes in the properties of the low-temperature L_1 states. Table XV gives the magnetic characteristics of the L_2 states. We can see that the magnetic properties of the L_2 states are practically unaffected throughout the investigated temperature range. However, as before, the negative difference between the Curie temperatures of the low-temperature L_2 and L_1 states is retained. As pointed out in the preceding subsections, this difference represents a reduction in the average value of the conduction electron density within a grain boundary compared with the bulk of the grains adjoining this boundary.

3.5. Conclusions

A fuller utilization of the capabilities of the atomic probe methodology has made it possible:

to develop a new method for obtaining microscopic information on the structure, electronic and dynamic properties of the cores of defects, such as grain boundaries and dislocations;

to determine independently the size of the cores of these defects in which the paths of accelerated migration of atomic probes are located: this size is approximately 10^{-8} cm;

TABLE XV.

Host lattice	Pd	Pt	Rh	Ir
T^{LT} (L_2)	120	90	45	60
ΔT (L_2)	—	0	—50	—20
H^{LT} (L_2)	275	270	150	50
ΔH (L_2)	—	—45	—40	—20
H^{LT}	0	0	0	0

to discover the unique state of atomic probes in recrystallization grain boundaries typical of a wide range of fcc and bcc metals;

to determine the characteristic temperature of the diffusion saturation of polycrystalline samples with atomic probes (triple point) at which there is a change in the mechanism of diffusion "pumping out" from the vacancy mechanism at high temperatures to the impurity–vacancy mechanism at low temperatures;

to develop a new method for investigating the properties of impurity segregation regions near grain boundaries based on the low-temperature L_1 states of atomic probes;

to discover a lower average value of the conduction electron density within the cores of grain boundaries and dislocations;

to determine a complex set of dynamic and electronic properties of atomic probes within grain boundaries, which can only be due to the participation of atomic probes in mixed split interstitials;

to discover magnetic phase transitions in two-dimensional regions, such as planes of grain boundaries and in monatomic layers of the regular lattice adjoining grain boundaries.

We shall now consider the most urgent tasks in the field of physical studies of the structure and properties of defects of the grain-boundary type, and we shall state only the most obvious.

Since many characteristics and properties of grain boundaries and adjoining regular lattice regions have been found because of the ferromagnetic phase transitions discovered by us, which occur in such regions in platinum, palladium, rhodium, and iridium, it is necessary to find alternative approaches to these lattices (matrices) in which the indirect exchange interaction of magnetically active impurities via conduction electrons does not take place.

The most urgent task is to obtain direct microscopic data on the mechanisms and characteristics of diffusion jumps within dislocation cores or in grain boundaries (in the L_2 states) deduced from the diffusion broadening of the NGR lines at high temperatures and from the anisotropy of the NGR probability under these conditions.

Obviously, the use of grain boundaries of different types in NGR experiments would provide a fresh approach to the relationship between the properties of grain boundaries and their atomic structure.

Finally, as mentioned already, changes in the composition of the whole polycrystalline sample or local changes in grain boundaries investigated by preferential grain-boundary diffusion should make it possible to investigate the influence of doping on all the grain boundary characteristics determined by the new method including their structure, electronic and dynamic properties, and microscopic diffusion parameters.

The author is deeply grateful to Academician S.V. Vonsovskiĭ for his continuous interest and encouragement, and for numerous discussions which stimulated the writing of this review.

[1]B. S. Bokshteĭn, Ch. V. Kopetskiĭ, and L. S. Shvindlerman, Grain Boundaries in Metals [in Russian], Nauka, M., 1984.
[2]G. Vogl, Phys. Status Solidi B **144**, 259 (1987).
[3]R. Sielemann, Mater. Sci. Forum **15–18**, 25 (1987).
[4]V. N. Kaĭgorodov and S. M. Klotsman, Pis'ma Zh. Eksp. Teor. Fiz. **28**, 386 (1978) [JETP Lett. **28**, 356 (1978)].
[5]V. N. Kaĭgorodov, S. M. Klotsman, and S. N. Shlyapnikov, Poverkhnost' No. 5, 57 (1982). [Phys. Chem. Mech. Surf. (1982)].
[6]V. N. Kaĭgorodov, S. M. Klotsman, and V. M. Koloskov, Fiz. Met. Metalloved. **63**, 614 (1987). [Phys. Met. Metallogr. (USSR) **63**(3), 186 (1987)].
[7]V. N. Kaigorodov, S. M. Klotsman, V. M. Koloskov, and S. N. Shlyapnikov, Poverkhnost' No. 3, 124 (1987). [Phys. Chem. Mech. Surf. (1987)].
[8]V. N. Kaĭgorodov, S. M. Klotsman, V. M. Koloskov, and G. N. Tatarinova, Fiz. Met. Metalloved. **66**, 958 (1988). [Phys. Met. Metallogr. (USSR) **66** (1988)].
[9]V. N. Kaĭgorodov, S. M. Klotsman, and S. N. Shlyapnikov, Fiz. Met. Metalloved. **66**, 200 (1988). [Phys. Met. Metallogr. (USSR) **66**, (1988)].
[10]V. N. Kaĭgorodof, S. M. Klotsman, V. M. Koloskov, and S. N. Shlyapnikov, Mater. Sci. Forum (in press).
[11]D. Lazarus, Phys. Rev. **93**, 973 (1953).
[12]A. D. LeClaire, J. Nucl. Mater **69–70**, 245 (1978).
[13]S. Ishioka, H. Nakajima, and M. Koiwa, Philos. Mag. A **55**, 359 (1987).
[14]M. Klotsman, I. P. Polikarpova, G. N. Tatarinova, and A. N. Timofeev, Phys. Rev. B **38**, 7765 (1988).
[15]T. Yu. Gol'dshteĭn, Author's Abstract of Thesis for Candidate's Degree [in Russian], Ural State University, Sverdlovsk (1951) [Unfortunately, a mathematical description of preferential grain-boundary diffusion given in this thesis, completely identical with that of Ref. 16, was never published].
[16]J. C. Fisher, J. Appl. Phys. **22**, 74 (1951).
[17]J. Kaur and W. Gust, *Fundamentals of Grain and Interphase Boundary Diffusion*, Ziegler Press, Stuttgart, West Germany, 1988.
[18]H. S. Levine and C. J. MacCallum, J. Appl. Phys. **31**, 595 (1960).
[19]J. T. Robinson and N. L. Peterson, Acta Metall. **21**, 1181 (1973).
[20]J. T. Robinson and N. L. Peterson, Surf. Sci. **31**, 586 (1972).
[21]V. N. Kaĭgorodov, S. M. Klotsman, A. N. Timofeev, and I. Sh. Trakhtenberg, Fiz. Met. Metalloved. **25**, 910 (1968). [Phys. Met. Metallogr. (USSR) **25**(5), 150 (1968)].
[22]V. N. Kaĭgorodov, S. M. Klotsman, A. N. Timofeev, and I. Sh. Trakhtenberg, Fiz. Met. Metalloved. **25**, 1099 (1968). [Phys. Met. Metallogr, (USSR) **25**(6), 143 (1968)].
[23]V. N. Kaĭgorodov, Ya. A. Rabovskiĭ, and V. K. Talinskiĭ. Fiz. Met. Metalloved. **24**, 661 (1967). [Phys. Met. Metallogr. (USSR) **24**(4), 78 (1967)].
[24]V. N. Kaĭgorodov, Ya. A. Rabovskiĭ, and V. K. Talinskiĭ, Fiz. Met. Metalloved. **24**, 117 (1967). [Phys. Met. Metallogr. (USSR) **24**(1), 115 (1967)].
[25]V. N. Kaĭgorodov, S. M. Klotsman, and A. N. Timofeev, Fiz. Met. Metalloved. **27**, 627 (1969). [Phys. Met. Metallogr. (USSR) **27**(4), 55 (1969)].
[26]V. N. Kaĭgorodov, S. M. Klotsman, A. N. Timofeev, and I. Sh. Trakhtenberg, Fiz. Met. Metalloved. **27**, 1048 (1969). [Phys. Met. Metallogr. (USSR) **27**(6), 91 (1969)].
[27]V. N. Kaĭgorodov, S. M. Klotsman, A. N. Timofeev, and I. Sh. Trakhtenberg, Fiz. Met. Metalloved. **28**, 120 (1969). [Phys. Met. Metallogr. (USSR) **28**(6), 128 (1969)].
[28]A. B. Vladimirov, V. N. Kaĭgorodov, S. M. Klotsman, and I. Sh. Trakhtenberg, Fiz. Met. Metalloved. **68**, 342 (1989). [Phys. Met. Metallogr. (USSR) **68** (1989)].
[29]J. Geise, H. Mehrer, C. Herzig, and G. Weyer, Mater. Sci. Forum **15–18**, 443 (1987).
[30]A. N. Orlov, V. N. Perevezentsev, and V. V. Rybin, *Grain Boundaries in Metals* [in Russian], Metallurgiya, 1980.
[31]P. Neuhaus and C. Herzig, Preprint, Universität Münster (1988).
[32]P. G. Shewmon, *Diffusion in Solids*, McGraw-Hill, N. Y., (1963).
[33]B. S. Bokshtein, *Diffusion in Metals* [in Russian], Metallurgiya, M., 1978.
[34]S. Fujita, J. Phys. Chem. Solids **49**, 41 (1988).
[35]D. Wolf, Philos. Mag. A **47**, 147 (1983).
[36]S. M. Klotsman, Ya. A. Rabovskiĭ, V. K. Talinskiĭ, and A. N. Timofeev, Fiz. Met. Metalloved. **28**, 1025 (1969). [Phys. Met. Metallogr. (USSR) **28**(6), 66 (1969)].
[37]S. M. Klotsman, Ya. A. Rabovskiĭ, V. K. Talinskiĭ, and A. N. Timofeev, Fiz. Met. Metalloved. **29**, 803 (1970). [Phys. Met. Metallogr. (USSR) **29**(4), 127 (1970)].
[38]S. M. Klotsman, Ya. A. Rabovskiĭ, V. K. Talinskiĭ, and A. N. Timofeev, Fiz. Met. Metalloved. **31**, 429 (1971). [Phys. Met. Metallogr. (USSR) **31**(2), 214 (1971)].
[39]V. A. Gorbachev, S. M. Klotsman, Ya. A. Rabovskiĭ, V. K. Talinskiĭ, and A. N. Timofeev, Fiz. Met. Metalloved. **34**, 879 (1972). [Phys. Met. Metallogr. (USSR) **34**(4), 202 (1972)].

[40]V. A. Gorbachev, S. M. Klotsman, Ya. A. Rabovskiĭ, V. K. Talinskiĭ, and A. N. Timofeev, Fiz. Met. Metalloved. **35**, 889 (1973). [Phys. Met. Metallogr. (USSR) **35**(4), 226 (1973)].
[41]V. A. Gorbachev, S. M. Klotsman, Ya. A. Rabovskiĭ, V. K. Talinskiĭ, and A. N. Timofeev, Fiz. Met. Metalloved. **44**, 214 (1977). [Phys. Met. Metallogr. (USSR) **44**(1), 191 (1977)].
[42]S. M. Klotsman, Ya. A. Rabovskiĭ, V. K. Talinskiĭ, and A. N. Timofeev, Fiz. Met. Metalloved. **45**, 1104 (1978). [Phys. Met. Metallogr. (USSR) **45**(5), 181 (1978)].
[43]A. B. Vladimirov, S. M. Klotsman, and I. Sh. Trakhtenberg, Fiz. Met. Metalloved. (in press). [[Phys. Met. Metallogr. (USSR) (in press)].
[44]S. Z. Bokshteĭn, S. T. Kishkin, Yu. M. Mishin, and Yu. M. Razumovskiĭ, Poverkhnost' No. 3, 119 (1986). [Phys. Chem. Mech. Surf. (1986)].
[45]P. Neuhaus and C. Herzig, Acta Metall. **35**, 881 (1987).
[46]P. Neuhaus, C. Herzig, and W. Gust, Acta Metall. **37**, 587 (1989).
[47]S. M. Klotsman, Mater. Sci. Forum (in press).
[48]N. Stefanou, A. Oswald, R. Zeller, and P. H. Dederichs, Phys. Rev. B **35**, 6911 (1987).
[49]D. Gupta, J. Appl. Phys. **44**, 4455 (1973).
[50]D. Gupta, Phys. Rev. B **7**, 586 (1973).
[51]D. Gupta, Thin Solid Films **25**, 231 (1975).
[52]S. M. Klotsman, N. K. Arkhipova, A. N. Timofeev, and I. Sh. Trakhtenberg, Fiz. Met. Metalloved. **20**, 390 (1965). [Phys. Met. Metallogr. (USSR) **20**(3) (1965)].
[53]J. S. Lee, K. Vieregge and C. Herzig, Preprint, Universitäte Münster (1988).
[54]G. Clark and J. P. Stark, J. Appl. Phys. **61**, 438 (1987).
[55]S. M. Klotsman, Fiz. Met. Metalloved. **55**, 297 (1983). [Phys. Met. Metallogr. (USSR) **55**(2), 82 (1983)].
[56]W. L. Trousdale, G. Longworth, and T. A. Kitchens, J. Appl. Phys. **38**, 922 (1967).
[57]S. Mukherjee and J. L. Moran-Lopez, Surf. Sci. **188**, L742 (1987).
[58]W. N. Cathey, J. Phys. F **8**, 315 (1978).
[59]G. Bemski, J. Danon, A. M. De Graaf, and X. A. DaSilva, Phys. Lett. **18**, 213 (1965).
[60]A. Svane, Phys. Rev. Lett. **60**, 2693 (1988).
[61]R. E. Watson and L. H. Bennett, Phys. Rev. B **17**, 3714 (1978).
[62]S. M. Klotsman, A. N. Timofeev, and I. Sh. Trakhtenberg, Fiz. Met. Metalloved. **23**, 357 (1967). [Phys. Met. Metallogr. (USSR) **23**(2), 63 (1967)].
[63]W. Schilling, J. Nucl. Mater. **69–70**, 465 (1978).
[64]K. Sassa, W. Petry, and G. Vogl, Philos. Mag. A **48**, 41 (1983).
[65]D. M. Wahl, W. Mansel, and J. Marangos, Radiat. Eff. **103**, 59 (1987).
[66]K. H. Steinmetz, G. Vogl, W. Petry, and K. Schroeder, Phys. Rev. B **34**, 107 (1986).
[67]S. V. Vonsovskii, Magnetism, 2 vols., Halsted, N. Y., (1975). [Russ. original, Nauka, M., 1971, p. 174.].
[68]C. Kostler, F. Faupel, and T. Hehenkamp, Scr. Metall. **20**, 1755 (1986).
[69]K. H. Westmacott, U. Dahmen, and M. J. Witcomb, Metall. Trans. A **17**, 807 (1986).
[70]L. A. Ugodnikova, V. M. Beĭlin, and Yu. N. Tsiovkin, Pis'ma Zh. Eksp. Teor. Fiz. **19**, 433 (1974) [JETP Lett. **19**, 234 (1974)].

Translated by A. Tybulewicz